

Stochastic modelling of symmetric positive-definite material tensors

Sharana Kumar Shivanand^{a,*}, Bojana Rosić^b, Hermann G. Matthies^a

^a *Institute of Scientific Computing, Technische Universität Braunschweig, Germany*

^b *Applied Mechanics and Data Analysis, University of Twente, The Netherlands*

Abstract

Spatial symmetries and invariances play an important role in the description of materials. When modelling material properties, it is important to be able to respect such invariances. Here we discuss how to model and generate random ensembles of tensors where one wants to be able to prescribe certain classes of spatial symmetries and invariances for the whole ensemble, while at the same time demanding that the mean or expected value of the ensemble be subject to a possibly ‘higher’ spatial invariance class. Our special interest is in the class of physically symmetric and positive definite tensors, as they appear often in the description of materials. As the set of positive definite tensors is not a linear space, but rather an open convex cone in the linear vector space of physically symmetric tensors, it may be advantageous to widen the notion of mean to the so-called Fréchet mean, which is based on distance measures between positive definite tensors other than the usual Euclidean one. For the sake of simplicity, as well as to expose the main idea as clearly as possible, we limit ourselves here to second order tensors. It is shown how the random ensemble can be modelled and generated, with fine control of the spatial symmetry or invariance of the whole ensemble, as well as its Fréchet mean, independently in its scaling and directional aspects. As an example, a 2D and a 3D model of steady-state heat conduction in a human proximal femur, a bone with high material anisotropy, is explored. It is modelled with a random thermal conductivity tensor, and the numerical results show the distinct impact of incorporating into the constitutive model different material uncertainties—scaling, orientation, and prescribed material symmetry—on the desired quantities of interest, such as temperature distribution and heat flux.

Keywords: stochastic material modelling, tensor-valued random variable, anisotropy, spatial symmetries of ensemble and mean, directional and scaling uncertainty, human proximal femur, uncertainty quantification

1. Introduction

Heterogeneous materials and their statistical description are of great interest in many fields. The properties of such materials often vary considerably on the spatial scales of interest, and additionally in many cases the material properties are only described statistically, reflecting some underlying uncertainty as to the exact values. This leads to the idea of a stochastic/random representation of these properties. The material properties are naturally collected in tensor quantities due to Curie’s principle on spatial symmetries

*Corresponding author. E-mail: s.shivanand@tu-bs.de

or invariances, and due to Onsager’s reciprocity relations [10]. These tensors are often of even order and physically symmetric—in elasticity this is often termed the *major* symmetry. Furthermore, when these tensorial properties appear in the definitions of stored energy or entropy production of stable systems, they are additionally positive definite. It is this class of even-order physically symmetric and positive definite (SPD) tensors which we are interested in describing. Well known examples of such tensors are the second-order tensors describing diffusion phenomena, mapping the gradient of some quantity to the flux of some related quantity, e.g. the thermal conductivity tensor mapping temperature gradients to fluxes of thermal energy. An example of fourth-order is the elasticity tensor of a linearly elastic material, which maps the strain tensor to the stress tensor. As the general idea of what we want to show can be explained easier and in a more intuitive way in the simplest non-trivial class of even-order tensors, namely the second-order tensors, we shall for the sake of simplicity and brevity limit ourselves to that case here. But the general idea applies to any even-order SPD tensor field.

Even though frequently the exact values of the tensorial entries may not be known, some properties resulting from general principles often are known; namely, often it is known what kind of symmetries or invariances are to be expected [37, 25]. These invariances—we shall prefer the term invariance over symmetry here to avoid confusion with the before mentioned physical symmetry, resp. the symmetry of the tensor as a linear mapping—under the operation of some symmetry group are well known, and here our focus is on point operations such as those defining isotropy. The number of such point groups is larger in the case of fourth-order tensors (e.g. [7, 5]) than in the case of second-order tensors [30], further re-enforcing our decision to limit ourselves here to second-order tensors for the sake of simplicity and clarity. And after a choice of bases, a second order tensor or linear transformation is represented by a matrix, so one may concentrate on symmetric positive definite matrices instead. We will switch to this representation whenever it is convenient to do so.

So what will be considered here are second-order SPD tensors with uncertainties, i.e. random SPD matrices, where certain invariances are known for the whole population. There is already quite a bit of previous work in this field, drawing on several sources, which will be reviewed only very cursory and briefly here. One such source is random matrix theory (e.g. [22]), as even-order tensors can always be viewed as linear mappings on the space of tensors of half the order by contracting over half the indices. By choosing a basis each such tensor can hence be represented by a matrix, and the class we are interested in can thus be represented by SPD matrices. Random SPD matrices arise in a number of fields, e.g. [39, 42] to name just two. As each SPD matrix can be spectrally decomposed and has orthogonal eigenvectors, random orthogonal matrices have some relevance here as well [31, 23, 33]. In particular—as will be shown—this allows the independent control of the strength (or size or norm) of the tensor and of its directional properties.

This identification of even-order tensors with linear maps also makes clear that even-order tensor(-field)s may be viewed as elements of a C^* -algebra [41, 43], with the vector space operations being obvious, and the multiplication corresponding to the concatenation of linear maps. This is the theoretical background for using functions of such tensor fields via spectral calculus. In our case the exponential function and its inverse, the logarithm, will be of prime importance. As these algebras in general are non-commutative, this affects the distributional properties of random elements of the algebra, and the prominent role of the Gaussian distribution in limit theorems has to be replaced by the circular distribution resp. the Wigner semicircle distribution [22].

A reduced non-parametric approach to generate random matrices is contained in [42], and based on this the generation of random elasticity tensors with known invariance in the mean and fully anisotropic invariance in each realisation is shown in a series of papers [17, 18, 19, 20, 21]. Here an algebraic property, namely that positive elements in the algebra are squares of other elements in the algebra, is used to ascertain that each generated tensor field is indeed SPD, and the theory of C^* -algebras ensures that each SPD tensor(-field) has a square root. Another example for a frequent approach to ensure the SPD property, based on spectral properties, is contained in e.g. [40]. This is a somewhat widely used technique when discussing diffusion and conductivity tensors, namely instead of describing the SPD tensor itself, one focuses with the description on its logarithm—and C^* -algebra theory assures us that a SPD tensor has a unique main-branch logarithm. To obtain the tensor, one finally takes the exponential, thus ensuring positive definiteness. We shall follow a similar path here.

The culmination of a long series of works [28, 38, 27, 26, 29] is reported in [30], which looks at stochastically homogeneous and isotropic random tensor fields of any order in a three dimensional domain. The results reported there allow a fine control about what invariance the mean of such a tensor field has, and what kind of invariance may be required of each realisation. Using the spectral theorem for the covariance of such homogeneous and isotropic fields and using the representation theory of the appropriate groups, here one may find the spectral resolution of the covariance function as well as a Karhunen-Loève like representation of the random tensor field with the desired invariance properties.

To recap, what is desired is a method to model and generate random material tensors that are symmetric and positive definite (SPD) in the sense of a mapping alluded to above, and that have a defined invariance under specified spatial symmetry groups, both for the mean or expected value, and for each single realisation. And if one uses the spectral decomposition to separate orientation and strength/size, then one has to be able to generate random orthogonal transformations. As regards the mean or expected value, questions arise about what is the *proper* or *adequate* mean to use. This is due to the fact that the usual arithmetic mean is wedded to a flat (vector-)space and a Euclidean distance. It is clear that on non-flat manifolds—e.g. the earth’s surface—a different metric than the Euclidean one of the ambient space has to be used, or to cite an example closer to our subject which will actually be used later, it is well known that the orthogonal transformations are a manifold, in fact a Lie group, and that gives it its own metric to compute distances and averages. Symmetric positive definite linear transformations, when viewed as a subset of the vector space of symmetric transformations, are geometrically an open cone, and they can be made into a Riemannian manifold in different ways with different metrics. The Fréchet or Karcher mean—the generalisation of the arithmetic mean to general metric spaces—defined using any of these non-Euclidean Riemannian metrics will therefore differ from the normal Euclidean or arithmetic mean [36].

In Section 2 we formulate the problem more precisely and spell out the desiderata for the modelling and generation of symmetric positive definite (SPD) matrices. As the spatial variation of homogeneous random fields is well known from the spectral decomposition of the corresponding correlation functions (e.g. [30]), and ensuring positive definiteness seems to be a main concern, we limit ourselves to spatially constant random tensor fields, i.e. random tensor variables. The spatial variation can easily be added as detailed in [30]. The modelling is then described in more detail in Section 3, first in the even simpler case in 2D, and then for 3D.

We also have an application in mind, which will be used in numerical examples to

demonstrate the workings of the different modelling assumptions. This is the thermal conductivity of bones [44, 8, 9] — a highly anisotropic material — which is important in some surgical procedures. It is described in Section 4. The results of the computations are shown in Sections 5 and 6, which then displays the effect on actual computational results of different modelling assumptions about the anisotropy. The Section 7 concludes.

2. Problem description

Let $\mathcal{G} \subset \mathbb{R}^d$ be a bounded domain in a d -dimensional Euclidean space \mathbb{R}^d (here $d = 2$ or $d = 3$), such that the behaviour of a physical system in the domain \mathcal{G} is governed by an abstract equation

$$\mathcal{A}(\mathbf{C}, \mathbf{u}) = \mathbf{f}. \quad (1)$$

Here $\mathbf{u} \in \mathcal{U}$ describes the state of the system lying in a Hilbert space \mathcal{U} (for the sake of simplicity), \mathcal{A} is a—possibly non-linear—operator modelling the physics of the system, and $\mathbf{f} \in \mathcal{U}^*$ is some external influence (action/excitation/loading).

Furthermore, the coefficient \mathbf{C} is regarded as a material tensor which represents intrinsic physics-based properties of materials, such as thermal conductivity, magnetic permeability, chemical diffusivity, and similar [37, 25]. It is modelled as a tensor-valued entity, taking values in the open convex cone of real-valued second order positive-definite tensors:

$$\text{Sym}^+(d) := \{\mathbf{C} \in (\mathbb{R}^d \otimes \mathbb{R}^d) \mid \mathbf{C} = \mathbf{C}^T, \mathbf{z}^T \mathbf{C} \mathbf{z} > \mathbf{0}, \forall \mathbf{z} \in \mathbb{R}^d \setminus \{\mathbf{0}\}\}. \quad (2)$$

As a simple example of Eq. (1), the reader may think of the well known thermal conduction equation — the example to be used in the numerical experiments:

$$-\nabla \cdot (\boldsymbol{\kappa}(x) \nabla T(x)) = f(x) \quad \forall x \in \mathcal{G}, \quad (3)$$

plus some appropriate boundary conditions on $\partial\mathcal{G}$. Here the system state is described by the temperature $T(\mathbf{x})$ at each point $\mathbf{x} \in \mathbb{R}^d$, the ‘loading’ $f(\mathbf{x})$ are thermal sinks and sources, and $\boldsymbol{\kappa}(x) \in \text{Sym}^+(d)$ is the second order tensor field of thermal conductivities. As already mentioned in Section 1, for the sake of simplicity we shall only deal with spatially constant random tensors, so that we would take here $\boldsymbol{\kappa}(x) \equiv \boldsymbol{\kappa} \in \text{Sym}^+(d)$.

Coming back to the general model Eq. (1), due to uncertainties in the exact value of \mathbf{C} , which may be due to a highly heterogeneous material, or simply a lack of knowledge about the exact value, we assume that a probabilistic model is adopted, so that it is modelled as a tensor-valued second order random variable, i.e. a mapping

$$\mathbf{C}(\omega) : \Omega \rightarrow \text{Sym}^+(d) \quad (4)$$

on a probability space $(\Omega, \mathfrak{F}, \mathbb{P})$, where Ω represents the sample space containing all outcomes $\omega \in \Omega$, \mathfrak{F} is the σ -algebra of measurable subsets of Ω , and \mathbb{P} is a probability measure. Similarly, one may assume the boundary or initial conditions, as well as external actions to be uncertain. However, this is secondary to the purpose of this paper and will not be covered further.

Evidently, this change transforms Eq. (1) to its stochastic counterpart, taking the form

$$\mathcal{A}(\mathbf{C}(\omega), \mathbf{u}(\omega)) = \mathbf{f}, \quad (5)$$

in which $\mathbf{u}(\omega)$ is a stochastic response, due to the randomness in $\mathbf{C}(\omega)$. Here we shall not be concerned on how this stochastic response may be computed, but primarily on how to

represent the symmetric positive definite (SPD) tensor $\mathbf{C}(\omega) \in \text{Sym}^+(d)$, which may be considered as a kind of parametrisation of that tensor-valued random variable.

One important point in the description of material properties of $\mathbf{C}(\omega) \in \text{Sym}^+(d)$ are symmetries in the sense of invariance against certain transformations. It is well known that the collection of all such transformations form a group G [10, 37, 30], and here we shall only be concerned with so-called point groups. Any such group $G \subseteq \text{O}(d)$ is a subgroup of the orthogonal group $\text{O}(d)$ of \mathbb{R}^d , and invariance here means that for all $\mathbf{R} \in G$ one has $\mathbf{R}^T \mathbf{C}(\omega) \mathbf{R} = \mathbf{C}(\omega)$. The set of tensors $\mathbf{C} \in \text{Sym}(d)$ which satisfy such an invariance are easily seen to form a subspace in $\text{Sym}(d)$ (e.g. [30]), the invariant subspace $\text{Sym}(d)_G \subseteq \text{Sym}(d)$ of the action of G . Hence the distribution of the $\mathbf{C}(\omega)$ lives only on this subspace, or more precisely on $\text{Sym}^+(d)_G := \text{Sym}^+(d) \cap \text{Sym}(d)_G$, as there will be no realisations outside of it. For the *mean* $\bar{\mathbf{C}}_\vartheta := \mathbb{E}_\vartheta(\mathbf{C}(\cdot))$, which is an averaging operation, it is possible (e.g. [30]) that it is invariant w.r.t. a larger group $G_m \supseteq G$. The kind of mean has not been specified as yet, it depends on how $\text{Sym}^+(d)$ is seen as a metric manifold with metric ϑ , and more about that will follow further below. This implies that $\bar{\mathbf{C}}_\vartheta \in \text{Sym}(d)_{G_m} \subseteq \text{Sym}(d)_G \subseteq \text{Sym}(d)$, as the G_m -invariant subspace $\text{Sym}(d)_{G_m}$ must be a subspace of the G -invariant subspace $\text{Sym}(d)_G$.

As to the description or parametrisation and generation of an SPD tensor-valued random variable $\mathbf{C}(\omega) \in \text{Sym}^+(d)_G$ to represent material properties, from the foregoing one thus has the following requirements:

- Each $\mathbf{C}(\omega)$ has to be symmetric, i.e. $\mathbf{C}(\omega) = \mathbf{C}^T(\omega) \in \text{Sym}(d)$.
- Even under numerical approximations like truncation of series resp. numerical quadrature, each $\mathbf{C}(\omega)$ has to be SPD, i.e. for all $\mathbf{z} \in \mathbb{R}^d \setminus \{\mathbf{0}\} : \mathbf{z}^T \mathbf{C}(\omega) \mathbf{z} > 0$.
- Each $\mathbf{C}(\omega) \in \text{Sym}^+(d)_G$ has to be invariant under some group of transformations $G \subseteq \text{O}(\mathbb{R}^d)$, the invariance or symmetry class of each realisation of the material.
- The mean $\bar{\mathbf{C}}_\vartheta := \mathbb{E}_\vartheta(\mathbf{C}(\cdot)) \in \text{Sym}^+(d)$ of the random tensor $\mathbf{C}(\omega)$ has to be invariant under some group of transformations G_m , where $G \subseteq G_m \subseteq \text{N}(G) \subseteq \text{O}(d)$; here G_m has to be ‘between’ the symmetry group G for each realisation and the normaliser subgroup $\text{N}(G) (= \{\mathbf{Q} \in \text{O}(d) \mid \forall \mathbf{R} \in G : \mathbf{Q} \mathbf{R} \mathbf{Q}^T \in G\})$, see also [30]).

The first item is not difficult to satisfy, as it is a simple linear constraint in $\mathfrak{gl}(d) := \mathbb{R}^d \otimes \mathbb{R}^d$, and $\text{Sym}(d) \subset \mathfrak{gl}(d)$ is a linear subspace. One may note that while $\dim(\mathfrak{gl}(d)) = d^2$, for the subspace $\text{Sym}(d)$ one only needs $\dim(\text{Sym}(d)) = d(d+1)/2$ parameters.

The second item, that each $\mathbf{C}(\omega)$ is SPD, can pose some problems, as $\text{Sym}^+(d) \subset \text{Sym}(d)$ is not a subspace, but geometrically an open convex cone. This means that still $\dim(\text{Sym}^+(d)) = d(d+1)/2$ parameters are needed, but they are not necessarily free resp. independent. In general, the third and fourth item can be satisfied by having an extended kind of Karhunen-Loève representation, which is displayed here for a general random tensor field $\mathbf{T}(\mathbf{x}, \omega)$ as a typically infinite series over the spectrum Λ —or an integral over $\lambda \in \Lambda$ in case of a continuous spectrum—of the covariance operator (here used with the usual arithmetic or Euclidean mean [30])

$$\mathbf{T}(\mathbf{x}, \omega) = \bar{\mathbf{T}}(\mathbf{x}) + \tilde{\mathbf{T}}(\mathbf{x}, \omega) = \sum_k c_k(\mathbf{x}) \mathbf{T}_k + \int_\Lambda \sum_\ell \varphi_\ell(\mathbf{x}, \lambda) \mathbf{Z}_\ell(d\lambda, \omega), \quad (6)$$

where $\bar{\mathbf{T}}(\mathbf{x}) = \sum_k c_k(\mathbf{x}) \mathbf{T}_k$ is the mean with the $\{\mathbf{T}_k\}$ a basis for the invariant subspace $\text{Sym}(d)_{G_m}$ of the action of G_m , and the zero-mean rest $\tilde{\mathbf{T}}(\mathbf{x}, \omega)$ is in a larger subspace

$\text{Sym}(d)_G \supseteq \text{Sym}(d)_{G_m}$, invariant under the action of $G \subseteq G_m$, where the $\text{Sym}(d)$ -valued random measures $\{\mathbf{Z}_\ell\}$ take their values in the G -invariant subspace $\text{Sym}(d)_G \subseteq \text{Sym}(d)$. By allowing possibly partly discrete measures \mathbf{Z}_ℓ , the general spectral integral over $\lambda \in \Lambda$ in Eq. (6) also includes sums and series.

If the above expression Eq. (6) were to be used for the SPD tensor $\mathbf{C}(\mathbf{x}, \omega) \in \text{Sym}^+(d)$, two problems might arise: one is that with Eq. (6) one is bound to the usual arithmetic or Euclidean mean, and the second one is that even though the expression Eq. (6) may guarantee—when exactly evaluated—that $\mathbf{C}(\mathbf{x}, \omega) \in \text{Sym}^+(d)$ is SPD, the sums may have to be truncated and the integrals may have to be approximated or evaluated numerically, and the guarantee evaporates in practical computations. As will be expanded on later, here we will propose instead of dealing with $\mathbf{C}(\mathbf{x}, \omega)$ directly to use and approximate $\mathbf{H}(\mathbf{x}, \omega) = \log \mathbf{C}(\mathbf{x}, \omega)$, which is free of the nonlinear SPD constraint. Once $\mathbf{H}(\mathbf{x}, \omega)$ has been approximated with the required invariance, one then may use $\mathbf{C} = \exp \mathbf{H}$ in the actual computation, which has the same invariances as \mathbf{H} .

In the approach [17, 18, 19, 20, 21], the problem of ensuring that each $\mathbf{C}(\mathbf{x}, \omega)$ is SPD is solved by representing the tensor as a square: the very definition of being positive in an algebra (like the C^* -algebra $\mathfrak{gl}(d)$) is that it is a generalised square, i.e. $\mathbf{C}(\mathbf{x}, \omega) = \mathbf{G}^T(\mathbf{x}, \omega) \mathbf{G}(\mathbf{x}, \omega)$, where $\mathbf{G}(\mathbf{x}, \omega) \in \text{GL}(d) \subset \mathfrak{gl}(d)$ has to be invertible—i.e. it has to be in the general linear group $\text{GL}(d)$. By choosing $\mathbf{G}(\mathbf{x}, \omega) \in \text{GL}(d)$ upper triangular, one is certain to use only $d(d+1)/2$ parameters, and the matrix $\mathbf{G}(\mathbf{x}, \omega)$ may be seen as a Cholesky-like factor of $\mathbf{C}(\mathbf{x}, \omega)$. By controlling the diagonal elements of the upper triangular matrix $\mathbf{G}(\mathbf{x}, \omega) \in \text{GL}(d)$, one can indeed make sure that it is invertible, and the otherwise troublesome nonlinear constraint of being non-singular becomes much simpler.

Although the authors in [17, 18, 19, 20, 21] make sure to allow the normal arithmetic or Euclidean mean

$$\mathbb{E}[\mathbf{C}(\mathbf{x}, \cdot)] = \int_{\Omega} \mathbf{C}(\mathbf{x}, \omega) \mathbb{P}(d\omega) \quad (7)$$

to have a symmetry class $G_m \subset O(d)$, the realisation of each random tensor itself is completely free in that it is not controlled for symmetries or invariances. On the other hand, in the approach in [30], there is refined attention to the invariances noted in the third and fourth requirement above, but no consideration is given for positive definiteness under approximation.

Also, both of these approaches only use the normal arithmetic mean Eq. (7). This is the mean one obtains by viewing $\text{Sym}^+(d) \subset \text{Sym}(d)$ simply as a subset of that vector space. One may recall here that interpolation and the mean or average are closely related on metric spaces, i.e. sets with a distance measure. After all, the mean or average of two items is midway between them on a shortest path—a geodesic, and along the geodesic one may interpolate between two items. Obviously a vector space like $\text{Sym}(d)$ with the usual Frobenius norm $\|\mathbf{C}\|_F^2 := \langle \mathbf{C}, \mathbf{C} \rangle_F := \text{tr}(\mathbf{C}\mathbf{C}^T)$ is a metric space with the usual Euclidean metric, and straight lines are geodesics, where one takes for the Euclidean metric $\vartheta_F(\mathbf{C}_1, \mathbf{C}_2) = \|\mathbf{C}_1 - \mathbf{C}_2\|_F$. On any such metric space with a metric ϑ , the Fréchet mean or average attached to that metric has a variational characterisation [36]: the simplest situation is one where there is a collection of n items $\{\mathbf{C}_1, \dots, \mathbf{C}_n\}$ with ‘weights’ or probabilities w_1, \dots, w_n , the mean or expected value is then defined as the minimiser of the ‘variance’:

$$\bar{\mathbf{C}}_\vartheta := \arg \min_{\hat{\mathbf{C}}} \sum_{k=1}^n w_k \vartheta(\hat{\mathbf{C}}, \mathbf{C}_k)^2, \quad (8)$$

with obvious generalisations for an infinite or even continuous collection. For general met-

ric spaces this is called the Fréchet mean, and for Riemannian manifolds also sometimes the Karcher mean [36]. If one uses the Frobenius metric ϑ_F on $\text{Sym}(d)$, one obtains the usual average resp. arithmetic or Euclidean mean.

Let us collect here some, in our view desirable, properties of a possible metric for material tensors $\mathbf{C}(\omega) \in \text{Sym}^+(d)$, which then may point to a certain kind of mean to use. From the point of physical modelling, if $\mathbf{C}(\omega)$ appears in a constitutive model, there is typically an inverse formulation involving $\mathbf{C}^{-1}(\omega)$. This means that one normally knows as much about the distribution of $\mathbf{C}(\omega)$ as about the distribution of $\mathbf{C}^{-1}(\omega)$, as the set $\text{Sym}^+(d)$ is stable under inversion. So one property of a desired metric ϑ_D on $\text{Sym}^+(d)$ would be invariance under inversion. Changing physical units would correspond to a scaling by a positive factor, so the desired metric should be invariant under scaling. And as a change of the coordinate system by an orthogonal transformation $\mathbf{R} \in \text{O}(d)$ changes the constitutive tensor \mathbf{C} to $\mathbf{R}^T \mathbf{C} \mathbf{R}$, one would like the desired metric ϑ_D to be invariant under such transformations. Collecting all together, the desiderata for a metric ϑ_D are then for all $\mathbf{C}_1, \mathbf{C}_2 \in \text{Sym}^+(d)$, $\alpha > 0$, and all $\mathbf{R} \in \text{O}(d)$:

- invariance under inversion: $\vartheta_D(\mathbf{C}_1^{-1}, \mathbf{C}_2^{-1}) = \vartheta_D(\mathbf{C}_1, \mathbf{C}_2)$;
- invariance under scaling: $\vartheta_D(\alpha \mathbf{C}_1, \alpha \mathbf{C}_2) = \vartheta_D(\mathbf{C}_1, \mathbf{C}_2)$;
- invariance under transformations: $\vartheta_D(\mathbf{R}^T \mathbf{C}_1 \mathbf{R}, \mathbf{R}^T \mathbf{C}_2 \mathbf{R}) = \vartheta_D(\mathbf{C}_1, \mathbf{C}_2)$.

The Frobenius distance satisfies the last requirement, but not the first two. Also, it is known from diffusion tensor imaging, that the straight line interpolation in the vector space $\text{Sym}(d)$ of two elements of $\text{Sym}^+(d)$ makes the interpolants ‘too fat’ (the so-called swelling effect [2, 39]), i.e. the determinant of the interpolant is comparatively too big. This short consideration shows that the normal arithmetic or Euclidean mean and expectation which results from the Frobenius distance is not ideal for SPD material tensors. In order not to distract the reader’s attention too much by reviewing different metrics used on $\text{Sym}^+(d)$, we relegate this material to [Appendix A](#).

What comes out of the considerations in [Appendix A](#) leads to the idea to be shown here in its simplest form, namely to ensure positive definiteness by using the isomorphism $\exp : \text{Sym}(d) \rightarrow \text{Sym}^+(d)$. This means to model $\mathbf{H} = \log(\mathbf{C}) \in \text{Sym}(d)$. As $\dim(\text{Sym}(d)) = d(d+1)/2$, this has the right number of parameters, and is free of any SPD constraints. The invariance requirements automatically translate to $\mathbf{H} = \log \mathbf{C}$, so that one may use the derivations from [30] such as Eq. (6) freely.

But here it is proposed to have an even finer control of orientation and ‘size’. This is achieved by looking at the spectral decomposition of a $\mathbf{C} \in \text{Sym}^+(d)$ and its logarithm $\mathbf{H} = \log(\mathbf{C})$:

$$\mathbf{C} = \mathbf{Q} \mathbf{\Lambda} \mathbf{Q}^T, \quad \log(\mathbf{C}) = \mathbf{Q} \log(\mathbf{\Lambda}) \mathbf{Q}^T = \mathbf{H} =: \mathbf{Q} \mathbf{Y} \mathbf{Q}^T, \quad (9)$$

with $\mathbf{Q} \in \text{SO}(d)$ and the diagonal matrix $\mathbf{\Lambda} = \text{diag}(\lambda^{(i)}) \in \text{Sym}^+(d)$ of positive eigenvalues $\{\lambda^{(i)} \mid i = 1, \dots, d\}$. Here the eigenvector matrix \mathbf{Q} controls the orientation, whereas the diagonal matrix $\mathbf{\Lambda}$ controls the scale or ‘size’ of the tensor \mathbf{C} , resp. the diagonal matrix $\mathbf{Y} = \text{diag}(y^{(i)}) = \text{diag}(\log(\lambda^{(i)})) = \log(\mathbf{\Lambda})$ controls the ‘size’ of $\mathbf{H} = \log \mathbf{C}$. By modelling $\mathbf{H} = \log(\mathbf{C}) \in \text{Sym}(d)$, one can control its ‘size’ and in turn that of $\mathbf{C} = \exp(\mathbf{H})$ by means of the free parameters $y^{(i)}$, without any regard of a positivity constraint like $\lambda^{(i)} > 0$.

By saying that we want to model $\mathbf{H} = \log(\mathbf{C})$, one has to be actually a bit more careful. The tensor \mathbf{C} has physical units, so that it does not directly make sense to

take its logarithm. What is meant by this is the following, without this always being addressed explicitly: taking a representative $\widehat{\mathbf{C}} = \widehat{\mathbf{Q}}\widehat{\boldsymbol{\Lambda}}\widehat{\mathbf{Q}}^T$ which has the right invariance properties—this could be the mean $\overline{\mathbf{C}}_\vartheta$ one wants to use—as a scaling, one may produce

$$\mathbf{C}(\omega) := \widehat{\mathbf{C}}^{1/2} \mathring{\mathbf{C}}(\omega) \widehat{\mathbf{C}}^{1/2}, \quad (10)$$

where $\widehat{\mathbf{C}}^{1/2} = \widehat{\mathbf{Q}}\widehat{\boldsymbol{\Lambda}}^{1/2}\widehat{\mathbf{Q}}^T$. The tensor $\mathring{\mathbf{C}}(\omega)$ may now be chosen dimensionless, so one may take its logarithm $\mathring{\mathbf{H}}(\omega) = \log(\mathring{\mathbf{C}}(\omega))$. In case $\widehat{\mathbf{C}} = \overline{\mathbf{C}}_\vartheta$ is really the mean, the tensor $\mathring{\mathbf{C}}(\omega)$ fluctuates around the identity, so that $\mathring{\mathbf{H}}(\omega)$ fluctuates around the origin.

3. Stochastic modelling

Looking at the relation Eq. (9) from the previous Section 2, we consider the analogous spectral decomposition of the deterministic representative tensor $\widehat{\mathbf{H}} = \log(\widehat{\mathbf{C}})$ —belonging to a predefined material symmetry into a real-valued diagonal matrix $\widehat{\mathbf{Y}} \in \text{Sym}(d)$, and the orthogonal normalised eigenvectors forming an orthogonal matrix $\widehat{\mathbf{Q}} \in \text{O}(d)$:

$$\widehat{\mathbf{H}} = \widehat{\mathbf{Q}}\widehat{\mathbf{Y}}\widehat{\mathbf{Q}}^T. \quad (11)$$

The above formulation may be used to model the deterministic material tensors that are used in everyday practice by generating $\widehat{\mathbf{H}}$ from Eq. (11) with the appropriate invariances, and then setting

$$\widehat{\mathbf{C}} = \exp(\widehat{\mathbf{H}}) = \widehat{\mathbf{Q}} \exp(\widehat{\mathbf{Y}}) \widehat{\mathbf{Q}}^T = \widehat{\mathbf{Q}} \exp(\text{diag}(\widehat{\mathbf{y}}^{(i)})) \widehat{\mathbf{Q}}^T = \widehat{\mathbf{Q}} \text{diag}(\mathbf{e}^{\widehat{\mathbf{y}}^{(i)}}) \widehat{\mathbf{Q}}^T, \quad (12)$$

which is guaranteed to be SPD by the properties of the exponential function.

To incorporate randomness in a tensor \mathbf{H} with fixed material symmetry, as a first step one may extend Eq. (11) and model the so-called scaling term $\widehat{\mathbf{Y}}$ as uncertain. We introduce a subscript s to signify the scaling uncertainty, and define the reference tensor $\widehat{\mathbf{H}}_s \in \text{Sym}(d)$ as

$$\widehat{\mathbf{H}}_s = \widehat{\mathbf{Q}}_s \widehat{\mathbf{Y}}_s \widehat{\mathbf{Q}}_s^T, \quad \text{and} \quad \widehat{\mathbf{C}}_s = \exp(\widehat{\mathbf{H}}_s). \quad (13)$$

The random tensor $\mathbf{H}_s(\omega_s) \in \text{Sym}(d)$ —accounting for random scaling only—then takes the form:

$$\mathbf{H}_s(\omega_s) = \widehat{\mathbf{Q}}_s \mathbf{Y}_s(\omega_s) \widehat{\mathbf{Q}}_s^T = \widehat{\mathbf{Q}}_s (\widehat{\mathbf{Y}}_s + \mathring{\mathbf{Y}}_s(\omega_s)) \widehat{\mathbf{Q}}_s^T, \quad (14)$$

so that, analogous to Eq. (12), one may compute $\mathbf{C}_s(\omega_s) = \exp(\mathbf{H}_s(\omega_s))$. The tensor $\mathbf{Y}_s(\omega_s) \in \text{Sym}(d)$ represents a stochastic diagonal matrix, assuming that $\mathbb{E}[\mathbf{Y}_s(\omega_s)] = \widehat{\mathbf{Y}}_s$ holds; here the usual arithmetic or Euclidean mean Eq. (7) is used, as we are free in the vector space of diagonal matrices in $\text{Sym}(d)$. Note that in case a scaling to dimensionless form like the one proposed in Eq. (10) has been carried out in such a way that $\widehat{\mathbf{C}}_s = \mathbb{E}_\vartheta(\mathbf{C}_s)$ is actually the mean, one has in terms of Eq. (10) that $\mathbb{E}_\vartheta(\mathring{\mathbf{C}}) = \mathbf{I}$.

In Eq. (14) in $\mathbf{Y}_s(\omega_s) = \text{diag}(\mathbf{y}_s^{(i)}(\omega_s))$, the d eigenvalues $\mathbf{y}_s^{(i)}$ of the tensor \mathbf{H}_s are free scalar real-valued random variables on a probability space $(\Omega_s, \mathfrak{F}_s, \mathbb{P}_s)$. As long as the distribution of $\mathring{\mathbf{Y}}_s(\omega_s) = \text{diag}(\mathring{\mathbf{y}}_s^{(i)}(\omega_s))$ is symmetric around the origin—meaning one knows as much about \mathbf{C} as about \mathbf{C}^{-1} , or more generally $\mathbb{E}(\mathring{\mathbf{Y}}_s) = \mathbf{0}$ with the usual arithmetic or Euclidean mean from Eq. (7)—in Eq. (10) one has $\mathbb{E}_\vartheta(\mathring{\mathbf{C}}) = \mathbf{I}$ with the Fréchet mean for the three metrics $\vartheta = \vartheta_G, \vartheta_L, \vartheta_S$ considered in Appendix A, and hence

$$\begin{aligned} \mathbb{E}_\vartheta(\mathbf{C}_s) &= \mathbb{E}_\vartheta(\exp(\mathbf{H}_s)) = \mathbb{E}_\vartheta(\exp(\widehat{\mathbf{Q}}_s \mathbf{Y}_s \widehat{\mathbf{Q}}_s^T)) = \mathbb{E}_\vartheta(\widehat{\mathbf{Q}}_s \exp(\mathbf{Y}_s) \widehat{\mathbf{Q}}_s^T) = \\ &= \widehat{\mathbf{Q}}_s \mathbb{E}_\vartheta(\exp(\mathbf{Y}_s)) \widehat{\mathbf{Q}}_s^T = \widehat{\mathbf{Q}}_s \exp(\widehat{\mathbf{Y}}_s) \widehat{\mathbf{Q}}_s^T = \exp(\widehat{\mathbf{Q}}_s \widehat{\mathbf{Y}}_s \widehat{\mathbf{Q}}_s^T) = \exp(\widehat{\mathbf{H}}_s) = \widehat{\mathbf{C}}_s \end{aligned} \quad (15)$$

with the Fréchet or Karcher mean for all three metrics.

Further, to model a specific invariance or material symmetry in the mean and each realisation, the correlation or dependence of the scaling random variables in Eq. (14) has to be mathematically described for each type of symmetry. For second order tensors, there are three types of invariance classes in 3D ($d = 3$), and two in 2D ($d = 2$) [30], depending on how many eigenvalues coincide.

Let us first consider the simpler case of 2D, where the tensor can be isotropic with two equal eigenvalues $y_s^{(1)} = y_s^{(2)}$ (a multiple of the identity), or orthotropic with distinct eigenvalues $y_s^{(1)} \neq y_s^{(2)}$, in which case the orthogonal matrix $\widehat{\mathbf{Q}}_s$ determines the directions of the major axes of the tensor. If in the first case one demands that each realisation is isotropic—and obviously also the reference $\widehat{\mathbf{C}}$ used in Eq. (10)—then only one random variable is needed to model both eigenvalues. On the other hand, if only the mean has to be isotropic but individual realisations may be orthotropic, then two independent identically distributed (iid) random variables could be used for the eigenvalues. Turning now to the case where the reference $\widehat{\mathbf{C}}$ is orthotropic, obviously one eigenvalue has to be larger than the other, say $\widehat{y}_s^{(1)} > \widehat{y}_s^{(2)}$. For the individual realisations, one may now choose to require that this relation holds also for each realisation, or only in the mean, together with some possible correlation of the eigenvalues. In case one wants to require this for each realisation with $y_s^{(1)} > y_s^{(2)}$, one trick to achieve this is to take two unconstrained random variables, say ξ_1 and ξ_2 , and set $y_s^{(2)} = \xi_1$ and $y_s^{(1)} = \xi_1 + \exp(\xi_2)$.

After this somewhat broad discussion of the 2D case, the 3D case may be treated in a similar way. The three invariance classes are determined again by the multiplicity of the eigenvalues, and the three cases are isotropy—all eigenvalues equal $y_s^{(1)} = y_s^{(2)} = y_s^{(3)}$ —or plan-isotropy, where two eigenvalues are equal (defining the plane of isotropy) and the third eigenvalue differs from these, or finally orthotropy, where all three eigenvalues are different. So it is possible to require that each realisation is plan-isotropic (or orthotropic), but that the mean is isotropic, or that each realisation may be orthotropic but the mean plan-isotropic (or isotropic).

The above discussed procedures emphasise only the modelling of the randomness in scaling parameters with fixed or varying material symmetry, while maintaining the directional attribute as deterministic. Nevertheless, it is a well known fact that anisotropic materials often also exhibit uncertainty in orientation due to the randomly oriented fibres/grains/crystals. The directional uncertainty in $\mathbf{H}(\omega)$ —by keeping the material symmetry constant—is incorporated by subjecting the eigenvectors in $\widehat{\mathbf{Q}}$ in Eq. (11) to random rotations. By using a subscript r (denoting the rotational uncertainty), the reference tensor $\widehat{\mathbf{H}}_r \in \text{Sym}(d)$ is therefore represented by rewriting Eq. (11) analogous to Eq. (13) as

$$\widehat{\mathbf{H}}_r = \widehat{\mathbf{Q}}_r \widehat{\mathbf{Y}}_r \widehat{\mathbf{Q}}_r^T, \quad \text{and} \quad \widehat{\mathbf{C}}_r = \exp(\widehat{\mathbf{H}}_r). \quad (16)$$

The stochastic tensor $\mathbf{H}_r(\omega_r) \in \text{Sym}(d)$ —with random orientation only—is then defined in the form:

$$\mathbf{H}_r(\omega_r) = \mathbf{R}(\omega_r) \widehat{\mathbf{H}}_r \mathbf{R}(\omega_r)^T = \mathbf{R}(\omega_r) \widehat{\mathbf{Q}}_r \widehat{\mathbf{Y}}_r \widehat{\mathbf{Q}}_r^T \mathbf{R}(\omega_r)^T, \quad (17)$$

—or equivalently $\mathbf{C}_r(\omega_r) = \mathbf{R}(\omega_r) \exp(\widehat{\mathbf{H}}_r) \mathbf{R}(\omega_r)^T = \mathbf{R}(\omega_r) \widehat{\mathbf{C}}_r \mathbf{R}(\omega_r)^T$, where $\mathbf{R} \in \text{SO}(d)$ is a random rotation matrix, chosen such that each realisation of $\mathbf{H}_r(\omega_r)$ resp. $\mathbf{C}_r(\omega_r)$ satisfies the appropriate invariance requirements.

It now becomes necessary to represent random rotations like $\mathbf{R}(\omega_r) \in \text{SO}(d)$; as there are very many approaches to represent rotations as well as a large amount of easily accessible literature, they will not be reviewed presently as this would lead the discussion

astray. In order to arrive at a vector space setting preferred by us, we resort to the well known correspondence between the Lie group $\text{SO}(d)$ of orthogonal matrices with unit determinant and its Lie algebra $\mathfrak{so}(d)$ of skew-symmetric matrices [34, 6], also alluded to in [Appendix A](#):

$$\mathbf{R} = \exp(\mathbf{W}) \in \text{SO}(d), \quad \text{and} \quad \mathbf{W} = \log(\mathbf{R}) \in \mathfrak{so}(d). \quad (18)$$

Of course, it will not be possible to establish a one-to-one relation between the Lie group $\text{SO}(d)$ and some real vector space, as $\text{SO}(d)$ is compact—this is easily seen in 2D where $\text{SO}(2)$ is homeomorphic to the one one-sphere resp. the unit circle in \mathbb{R}^2 , or in 3D where the representation through unit quaternions shows that $\text{SO}(3)$ is homeomorphic to the three-sphere resp. the unit sphere in \mathbb{R}^4 —and a real vector space is not compact. But the relations in Eq. (18) come pretty close to this desideratum, which makes the probabilistic modelling quite a bit easier.

Especially in 3D one may use an explicit version of Eq. (18), the well-known Rodrigues rotation formula, e.g. [6]. There is a familiar correspondence between a skew-symmetric matrix $\mathbf{W} \in \mathfrak{so}(3)$ and the defining Euler vector $\mathbf{w} = [w_1, w_2, w_3]^T \in \mathbb{R}^3$ along its unit rotation axis vector $\mathbf{v} = \mathbf{w}/\|\mathbf{w}\|$

$$\mathbf{W} = \begin{bmatrix} 0 & -w_3 & w_2 \\ w_3 & 0 & -w_1 \\ -w_2 & w_1 & 0 \end{bmatrix}, \quad (19)$$

which is the unique rotation axis of a non-trivial rotation \mathbf{R} with rotation angle $\phi = \|\mathbf{w}\|$. Rodrigues's rotation formula may then be written as

$$\mathbf{R} = \exp(\mathbf{W}) = \mathbf{I} + \frac{\sin \phi}{\phi} \mathbf{W} + \frac{1 - \cos \phi}{\phi^2} \mathbf{W}^2 = \mathbf{I} + \frac{\sin \phi}{\phi} \mathbf{W} + 2 \frac{\sin^2(\phi/2)}{\phi^2} \mathbf{W}^2, \quad (20)$$

and inversely [13]

$$\mathbf{W} = \frac{\arcsin \alpha}{\alpha} \mathbf{S} \quad \text{with} \quad \mathbf{S} = \frac{1}{2}(\mathbf{R} - \mathbf{R}^T) \quad \text{and} \quad \alpha = \sqrt{\frac{1}{2} \text{tr}(\mathbf{S}\mathbf{S}^T)}. \quad (21)$$

Note that obviously in the case $d = 2$ the axis of rotation \mathbf{w} is fixed perpendicular to the plane; only the rotational angle $\phi(\omega_r)$ is modelled as a circular/angular random variable [31, 23]. On the other hand, when $d = 3$, the defining vector $\mathbf{w}(\omega_r)$ is a \mathbb{R}^3 -valued random vector with values in the ball with radius π , and the random angle of rotation is $\phi(\omega_r) = \|\mathbf{w}(\omega_r)\|$, defined on a probability space $(\Omega_r, \mathfrak{F}_r, \mathbb{P}_r)$. In any case one obtains a random $\mathbf{R}(\omega_r) \in \text{SO}(d)$. Again, as long as the distribution of $\mathbf{w}(\omega_r)$ resp. $\phi(\omega_r)$ is symmetric around the origin or rather $\mathbb{E}(\mathbf{w}) = \mathbf{0}$ resp. $\mathbb{E}(\phi) = 0$, the expected value of $\mathbf{R}(\omega_r)$ of the here adequate Fréchet or Karcher mean with the metric ϑ_R (defined in [Appendix A](#)) is the identity, $\mathbf{I} = \mathbb{E}_{\vartheta_R}(\mathbf{R})$. Hence, like in Eq. (15), one has also in this case

$$\mathbb{E}_{\vartheta_S}(\mathbf{C}_r) = \mathbb{E}_{\vartheta_S}(\mathbf{R} \exp(\widehat{\mathbf{H}}_r) \mathbf{R}^T) = \exp(\widehat{\mathbf{H}}_r) = \widehat{\mathbf{C}}_r. \quad (22)$$

To account for both random orientation and scaling attributes in the tensor \mathbf{H} , one may combine the two approaches. If these two aspects are considered independent, one may define the probability space as a product space $(\Omega, \mathfrak{F}, \mathbb{P})$ with $\Omega := \Omega_s \times \Omega_r$, $\mathfrak{F} := \mathfrak{F}_s \otimes \mathfrak{F}_r$, and a product measure $\mathbb{P} := \mathbb{P}_s \otimes \mathbb{P}_r$. In any case, denoting a combined rotational-scaling uncertainty with a subscript rs , and reusing the already defined subscripts from Eqs. (13) and (16), the reference tensor

$$\widehat{\mathbf{H}}_{rs} = \widehat{\mathbf{Q}}_r \widehat{\mathbf{Y}}_s \widehat{\mathbf{Q}}_r^T, \quad \text{as well as} \quad \widehat{\mathbf{C}}_{rs} = \exp(\widehat{\mathbf{H}}_{rs}), \quad (23)$$

is turned a stochastic tensor by incorporating both the directional and scaling uncertainties in the following manner:

$$\mathbf{H}_{rs}(\omega) = \mathbf{R}(\omega_r) \widehat{\mathbf{Q}}_r \mathbf{Y}_s(\omega_s) \widehat{\mathbf{Q}}_r^T \mathbf{R}(\omega_r)^T, \quad (24)$$

or equivalently

$$\mathbf{C}_{rs}(\omega) = \exp(\mathbf{H}_{rs}(\omega)) = \mathbf{R}(\omega_r) \widehat{\mathbf{Q}}_r \exp(\mathbf{Y}_s(\omega_s)) \widehat{\mathbf{Q}}_r^T \mathbf{R}(\omega_r)^T. \quad (25)$$

In this manner, one may expand now the previous possibilities with a given invariance or symmetry class for the mean, by allowing the random part to not only vary in scaling in a defined invariance or symmetry class as previously considered, but the orientation of the invariance or symmetry class of the random part may also be considered as uncertain, and this randomness modelled as just described.

Again, if as considered before, the model is such $\mathbb{E}_{\vartheta_R}(\mathbf{R}) = \mathbf{I}$ and $\mathbb{E}(\mathbf{Y}_s) = \widehat{\mathbf{Y}}_s$, and if one assumes a product measure $\mathbb{P} := \mathbb{P}_s \otimes \mathbb{P}_r$, then, like in Eqs. (15) and (22), one has here again from Eq. (25)

$$\mathbb{E}_{\vartheta_S}(\mathbf{C}_{rs}) = \mathbb{E}_{\vartheta_S}(\mathbf{R} \widehat{\mathbf{Q}}_r \exp(\mathbf{Y}_s) \widehat{\mathbf{Q}}_r^T \mathbf{R}^T) = \exp(\widehat{\mathbf{H}}_{rs}) = \widehat{\mathbf{C}}_{rs}. \quad (26)$$

One may observe that the ϑ_S metric is well suited to this kind of model, and thus the calculation of the associated Fréchet or Karcher mean gives such simple results. The other possible means with the ϑ_G or with the ϑ_L metric will be somehow deformed when adding in rotational uncertainty, as will the usual resp. arithmetic or Eulidean mean, which is further explored in [Appendix B](#).

4. Application to steady-state heat conduction

Referring to the deterministic model of heat conduction defined in Eq. (3), let the conductivity tensor $\boldsymbol{\kappa} \in \text{Sym}^+(d)$ be modelled as a random tensor as described in Eq. (24). The scaling terms $\boldsymbol{\Lambda}_s = \text{diag}(\lambda_s^{(i)}) \in \text{Sym}^+(d)$ of the tensor $\boldsymbol{\kappa}$ are modelled as positive log-normal random variables:

$$\boldsymbol{\Lambda}_s(\omega_s) = \text{diag}(\lambda_s^{(i)}(\omega_s)) = \exp(\mathbf{Y}_s(\omega_s)) = \text{diag}(\exp(y_s^{(i)}(\omega_s))), \quad (27)$$

i.e. a non-linear transformation of the Gaussian random variables

$$y_s^{(i)}(\omega_s) \sim \mathcal{N}(\mu_i, \sigma_i), \quad i = 1, \dots, d, \quad (28)$$

where the parameters $\{\mu_i\}_{i=1}^d \in \mathbb{R}$ and $\{\sigma_i\}_{i=1}^d \in \mathbb{R}^+$ denote the mean and standard deviation corresponding to the Gaussian distribution.

Further, the directional uncertainty of $\boldsymbol{\kappa}$ is accounted by constructing the random rotation matrix $\mathbf{R}(\omega_r)$ as given in Eq. (20). This is accomplished by modelling the unit axis vector $\mathbf{v}(\omega_r)$ as a von Mises-Fisher distribution defined on the unit sphere \mathbb{S}^2 [31], and subsequently, by determining the random rotational angle $\phi(\omega_r)$. If one of the eigenvectors of the matrix $\widehat{\mathbf{Q}}_r$ represents the mean direction $\boldsymbol{\mu}_{\text{circ}} \in \mathbb{S}^2$ of the von Mises-Fisher vector $\mathbf{v}(\omega_r)$, then the corresponding probability density function (PDF) takes the form:

$$f(\mathbf{v}(\omega_r) | \boldsymbol{\mu}_{\text{circ}}, \eta) = \frac{\eta^{d/2-1}}{(2\pi)^{d/2} \mathcal{I}_{d/2-1}(\eta)} \exp(\eta \boldsymbol{\mu}_{\text{circ}}^T \mathbf{v}(\omega_r)), \quad (29)$$

where $\eta \in \mathbb{R}^+$ is the measure of concentration, and \mathcal{I}_p is the modified Bessel function of order p . When $d = 2$, as only the rotational angle $\phi(\omega_r)$ is modelled as a random variable on the unit circle \mathbb{S}^1 , the above PDF reduces to the von Mises distribution [4]:

$$f(\phi(\omega_r)|\bar{\phi}, \eta) = \frac{\exp(\eta \cos(\phi(\omega_r) - \bar{\phi}))}{2\pi \mathcal{I}_0(\eta)}, \quad (30)$$

in which $\bar{\phi}$ is the mean direction of the von Mises circular random variable $\phi(\omega_r)$.

By rewriting the deterministic model in Eq. (3) to a stochastic one

$$-\nabla \cdot (\boldsymbol{\kappa}(\omega) \nabla T(\mathbf{x}, \omega)) = f(\mathbf{x}) \quad \forall \mathbf{x} \in \mathcal{G}, \omega \in \Omega, \quad (31)$$

the goal is to determine the random temperature field $T(\mathbf{x}, \omega) : \mathcal{G} \times \Omega \rightarrow \mathbb{R}$, assuming deterministic boundary conditions and heat source.

Given the weak form of Eq. (31), we use the finite element method to seek for an approximate solution $T_h(\mathbf{x}, \omega)$ on a finite-dimensional subspace $\mathcal{U}_h \subset \mathcal{U}$ of the solution space \mathcal{U} of Eq. (3), where as usual h is the discretisation parameter—an indicator of element size. Subsequently, the objective of this study is to determine the statistics like the mean and standard deviation of the solution $T_h(\mathbf{x}, \omega)$ using the classical Monte Carlo method (MC) [32, 14]. Given, i.i.d. $\{\boldsymbol{\kappa}(\omega_i)\}_{i=1}^N$ samples, where N is the sample size, one may compute the statistics of discretised solution $T_{h,N} := \{T_h(\mathbf{x}, \omega_i)\}_{i=1}^N$. The unbiased sample mean [11] is then calculated as

$$\mu^{(\text{MC})}(T_{h,N}) := \frac{1}{N} \sum_{i=1}^N T_h(\mathbf{x}, \omega_i), \quad (32)$$

and the corrected sample standard deviation as

$$\text{Std}^{(\text{MC})}(T_{h,N}) := \sqrt{\frac{1}{N-1} \sum_{i=1}^N (T_h(\mathbf{x}, \omega_i) - \mu^{(\text{MC})}(T_{h,N}))^2}. \quad (33)$$

Along with the temperature field, we also evaluate the heat flux vector field $\mathbf{q}(\mathbf{x}, \omega) : \mathcal{G} \times \Omega \rightarrow \mathbb{R}^d$, whose approximate solution $\mathbf{q}_h(\mathbf{x}, \omega)$ is determined on a finite-dimensional subspace $\mathcal{V}_h \subset \mathcal{V}$, where \mathcal{V} is the solution space of heat flux, $\mathbf{q}(\mathbf{x}) = \boldsymbol{\kappa} \nabla T(\mathbf{x})$. Further, we determine the second order statistics of the magnitude of approximate heat flux vector field in the Euclidean norm i.e. $q_h^{(t)}(\mathbf{x}, \omega) = \|\mathbf{q}_h(\mathbf{x}, \omega)\|$. More specifically, the statistics such as the mean and standard deviation are obtained by sampling based MC estimators $\mu^{(\text{MC})}(q_{h,N}^{(t)})$ and $\text{Std}^{(\text{MC})}(q_{h,N}^{(t)})$, respectively.

Apart from evaluating the statistics of magnitude of heat flux field $\mathbf{q}_h(\mathbf{x}, \omega)$, one may also be interested in understanding the statistics of direction of heat flow. To this, one may compute the second order circular statistics of the normalized heat flux, $\hat{\mathbf{q}}_h(\mathbf{x}, \omega) = \mathbf{q}_h(\mathbf{x}, \omega)/q_h^{(t)}(\mathbf{x}, \omega)$. Subsequently, the MC mean estimate of the sampled unit vector field $\hat{\mathbf{q}}_{h,N} := \{\hat{\mathbf{q}}_h(\mathbf{x}, \omega_i)\}_{i=1}^N$ can be estimated accordingly [31, 23]:

$$\boldsymbol{\mu}^{(\text{MC})}(\hat{\mathbf{q}}_{h,N}) = \frac{1}{N} \sum_{i=1}^N \hat{\mathbf{q}}_h(\mathbf{x}, \omega_i) = L \boldsymbol{\mu}_{\text{circ}}^{(\text{MC})}(\hat{\mathbf{q}}_{h,N}), \quad (34)$$

where $L = \|\boldsymbol{\mu}^{(\text{MC})}(\hat{\mathbf{q}}_{h,N})\|$ represents resultant Euclidean length of the sample mean $\boldsymbol{\mu}^{(\text{MC})}(\hat{\mathbf{q}}_{h,N}) \in \mathbb{R}^d$, and $\boldsymbol{\mu}_{\text{circ}}^{(\text{MC})}(\hat{\mathbf{q}}_{h,N}) = \boldsymbol{\mu}^{(\text{MC})}(\hat{\mathbf{q}}_{h,N})/\|\boldsymbol{\mu}^{(\text{MC})}(\hat{\mathbf{q}}_{h,N})\|$ is a unit vector defining the sample mean direction of $\hat{\mathbf{q}}_{h,N}$. With the help of the former one, the sample circular standard deviation of $\hat{\mathbf{q}}_{h,N}$ can further be evaluated as

$$\text{Std}_{\text{circ}}^{(\text{MC})}(\hat{\mathbf{q}}_{h,N}) = \sqrt{-2 \log L}. \quad (35)$$

5. Results on 2D proximal femur

A two-dimensional proximal femur with a body of approximately 7 cm in width and 21.7 cm in height is considered, see Fig. 1. A uniformly distributed surface heat flux with a resultant heating of 0.1 W and a fixed temperature of 0 °C are applied at locations as shown in Fig. 1 [8]. The computational domain is discretized by the finite element discretization method with four-noded plane-stress elements, see Table 1 for the mesh specifications. In this study, each deterministic simulation obtained by sampling stochastic parametric space is solved by the Calculix solver [12]. For MC simulation, the Karl Pearson coefficient of dispersion $\delta = 0.1$ (for scaling uncertainty) and $N = 10^5$ samples are considered for all the cases in this study.

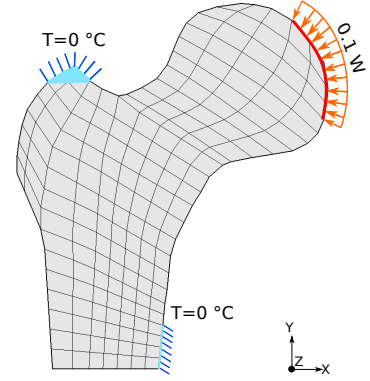


Figure 1: Boundary conditions of 2D femur bone

Elements	Nodes	Degrees of freedom
171	206	390

Table 1: Mesh specifications of 2D femur

For simplification, we use abbreviations defined in Table 2 which are used to refer different modelling scenarios considered in this study. Each model will have a unique name in the form: reference tensor symmetry-realisation symmetry-type of model. For instance, iso-ortho-scl represents a model with random scaling only, such that the reference tensor belongs to isotropic symmetry, whereas the realisations are of orthotropic symmetry. Three such possible scenarios are explored in this article—iso-iso-scl (isotropy-isotropy-random scaling), iso-ortho-scl (isotropy-orthotropy-random scaling) and ortho-ortho-dir (orthotropy-orthotropy-random direction). Consequently, using the subscripts

Mean/realisation symmetry		Type of model	
isotropy	orthotropy	random scaling	random direction
iso	ortho	scl	dir

Table 2: Model abbreviations

defined in Section 3 for random scaling and random orientation, two reference conductivity tensors— $\hat{\kappa}_s^{iso} \in \text{Sym}^+(2)$ belonging to isotropic symmetry (denoted by superscript *iso*) and $\hat{\kappa}_r^{ortho} \in \text{Sym}^+(2)$ with orthotropic symmetry (with superscript *ortho*)—are considered, whose values are tabulated in Table 3 [9]. Furthermore, we simulate the grain orientations of the femur in a spatially homogeneous sense. As a result, the eigenvectors of the tensor $\hat{\kappa}_r^{ortho}$ corresponding to the eigenvalues $\hat{\lambda}_r^{(1)}$ and $\hat{\lambda}_r^{(2)}$ are oriented at an angle of $\pi/4$ in a clockwise direction to the x and y-axis, respectively.

isotropy [W/m·K] $\hat{\kappa}_s^{iso}$	orthotropy [W/m·K] $\hat{\kappa}_r^{ortho}$
$\begin{bmatrix} 0.54 & 0 \\ 0 & 0.54 \end{bmatrix}$	$\begin{bmatrix} 0.77 & 0.23 \\ 0.23 & 0.77 \end{bmatrix}$
Eigenvalues [W/m·K]	
$\hat{\lambda}_s^{(1)} = 0.54,$ $\hat{\lambda}_s^{(2)} = 0.54$	$\hat{\lambda}_r^{(1)} = 0.54,$ $\hat{\lambda}_r^{(2)} = 1$

Table 3: Reference conductivity tensors with corresponding eigenvalues of 2D femur

Random scaling with fixed symmetry: the first modelling scenario is the one in which we perform random scaling only, such that the reference tensor $\hat{\kappa}_s^{iso}$, as well as the realisations, belong to isotropic symmetry (denoted by iso-iso-scl); see Fig. 2 for schematic overview of the model. In such a case, we model a random tensor $\kappa_s(\omega_s) \in \text{Sym}^+(2)$ —the exponential of the model depicted in Eq. (14)—with random scaling only. Here the uncertain scaling parameters $\lambda_s^{(1)}(\omega_s) = \lambda_s^{(2)}(\omega_s)$ are modelled as identical and dependent log-normal random variables. Their corresponding PDFs are shown in Fig. 2(a). A geometrically equivalent (circular) representation of reference tensor and realisations $\{\kappa_s(\omega_{s_i})\}_{i=1}^N \equiv \{\kappa_{s_i}\}_{i=1}^N$, where the radius of circle is defined by $1/\sqrt{\lambda_s^{(1)}(\omega_s)}$ and $1/\sqrt{\lambda_s^{(2)}(\omega_s)}$ [25], is presented in Fig. 2(b). As can be seen the preservation of isotropic symmetry is apparent given the constant circular shape among the random variable realisations. However, the varying size of circles signifies a variation in scaling parameters.

Random scaling with varying symmetry: in the next scenario, we consider a similar stochastic tensor $\kappa_s(\omega_s) \in \text{Sym}^+(2)$ as described previously with a similar reference tensor $\hat{\kappa}_s^{iso}$. The difference being that the eigenvalues $\{\lambda_s^{(i)}(\omega_s)\}_{i=1}^2$ are modelled as identical but independent (i.i.d) log-normal random variables. Due to which, the realisations of model $\kappa_s(\omega_s)$ belong to orthotropic symmetry, thus, this model is denoted as iso-ortho-scl. Furthermore, in orthotropic realisations, the eigenvectors of $\kappa_s(\omega_s)$ related to random eigenvalues $\lambda_s^{(1)}(\omega_s)$ and $\lambda_s^{(2)}(\omega_s)$ are constrained at an angle of $\pi/4$ in clockwise direction with respect to x and y-axis respectively. The schematic representation of this model with varying symmetry is displayed in Fig. 3, in which the corresponding PDFs are shown in Fig. 3(a). Closer inspection of the Fig. 3(b) shows the shift from circular geometry of isotropic reference tensor to orthotropic elliptical shape in realisations. One may also notice the variation in size of ellipses in the realisations as the semi-axes of ellipse are determined by $1/\sqrt{\lambda_s^{(1)}(\omega_s)}$ and $1/\sqrt{\lambda_s^{(2)}(\omega_s)}$.

Random orientation with fixed symmetry: in the last modelling scenario, we build a random tensor $\kappa_r(\omega_r) \in \text{Sym}^+(2)$, i.e. the exponential mapping of stochastic tensor as shown in Eq. (17), with random orientation only, given the reference tensor $\hat{\kappa}_r^{ortho}$. Here the model is designated as ortho-ortho-dir, since, a fixed orthotropic symmetry is preserved in mean and realisations. The random angle of rotation $\phi(\omega_r)$ is modelled as a von Mises random variable (see Eq. (30)) with zero mean $\bar{\phi} = 0$ with respect to x-axis and concentration parameter $\eta = 75$. In Fig. 4(a), the PDF $f(\phi(\omega_r))$ is shown on a real line over the domain $(-\pi, \pi]$, whereas the realisations of random variable $\phi(\omega_r)$ and its sample mean vector (solid straight line) are plotted on a unit circle in Fig. 4(b). In this

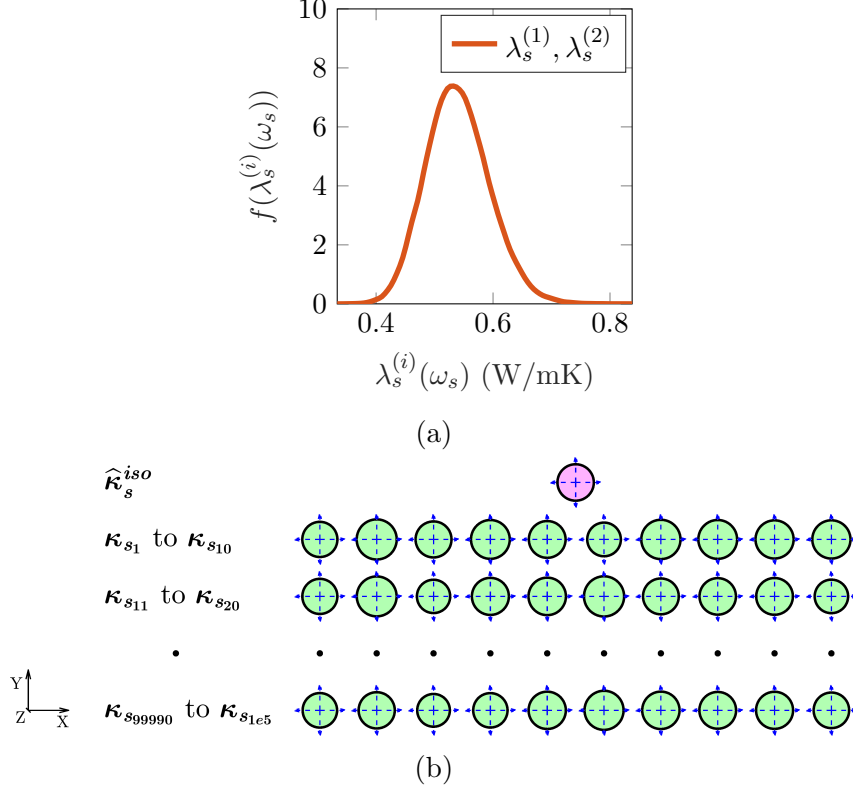


Figure 2: Stochastic tensor $\kappa_s(\omega_s)$ with fixed symmetry (iso-iso-scl): (a) log-normal PDF of identical and dependent random scaling values $\lambda_s^{(1)}(\omega_s) = \lambda_s^{(2)}(\omega_s)$, (b) geometric visualization of reference tensor $\hat{\kappa}_s^{iso}$ and realisations of random tensor $\kappa_s(\omega_s)$; the geometries are enhanced by scaling the eigenvalues by a factor of 0.5

study, we model directional uncertainty on the $x - y$ plane with z as the axis of rotation. Thereby, the corresponding random rotation matrix $\mathbf{R}(\omega_r)$ in Eq. (17) takes the form:

$$\mathbf{R}(\omega_r) = \begin{bmatrix} \cos \phi(\omega_r) & -\sin \phi(\omega_r) \\ \sin \phi(\omega_r) & \cos \phi(\omega_r) \end{bmatrix}. \quad (36)$$

Here we consider a right-handed Cartesian coordinate system, meaning that positive values of random variable $\phi(\omega_r)$ indicate counterclockwise rotation and vice versa. Fig. 4(c) depicts the corresponding elliptical geometric visualization of the model. As can be seen that the orientation of elliptical semi-axes fluctuates in the realisations $\{\kappa_r(\omega_{r_i})\}_{i=1}^N \equiv \{\kappa_{r_i}\}_{i=1}^N$, whereas its size and shape remain constant in the mean and realisations.

Uncertainty quantification: Fig. 5 shows the MC mean estimate of nodal temperature (NT) $T_{h,N}$ for the three described stochastic models. For easier interpretation, in this study, the results are displayed on a uniform scale. Hence, the values range from zero to a maximum value (corresponding to a given estimate of the desired output quantity). Clearly, the results in Figs. 5(a) and 5(b) are similar, as the considered reference tensor $\hat{\kappa}_s^{iso}$ is identical in both the cases. Due to the assumption of an orthotropic mean tensor $\hat{\kappa}_r^{ortho}$, in the third figure Fig. 5(c), we see a significant difference in the magnitude/contour pattern of temperature.

Fig. 6 further depicts the standard deviation of temperature $T_{h,N}$. Due to different modelling assumptions, it is apparent that all three results in this figure are different from each other. But Fig. 6(c) stands out the most, where the stochastic influence on nodal

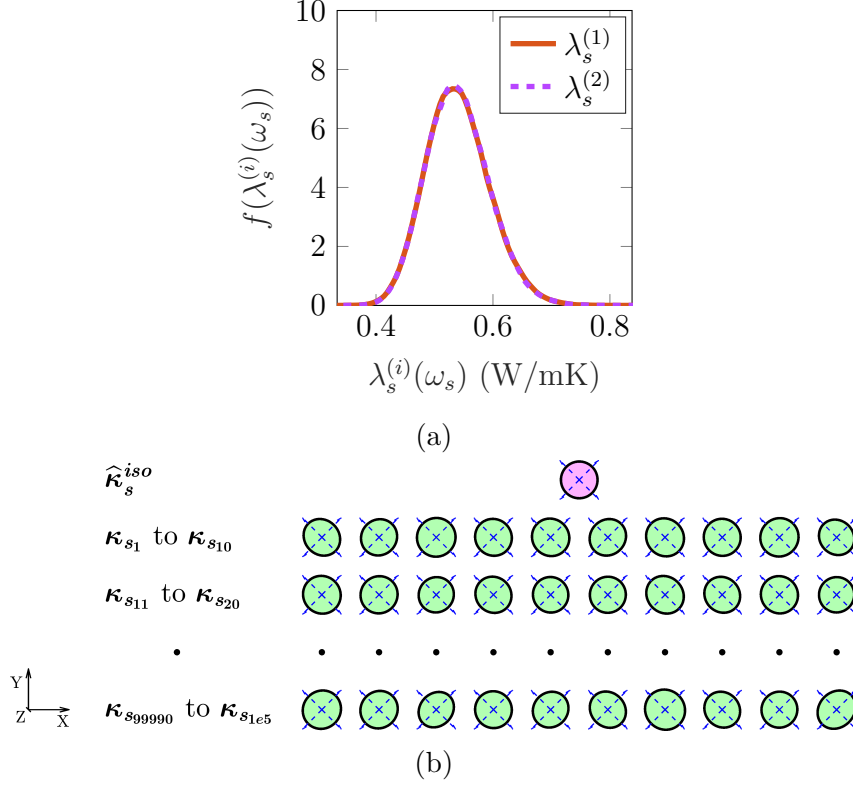


Figure 3: Stochastic tensor $\kappa_s(\omega_s)$ with varying symmetry (iso-ortho-scl): (a) log-normal PDF of i.i.d random scaling values $\{\lambda_s^{(i)}(\omega_s)\}_{i=1}^2$, (b) geometric visualization of reference tensor $\hat{\kappa}_s^{iso}$ and realisations of random tensor $\kappa_s(\omega_s)$; the geometries are enhanced by scaling the eigenvalues by a factor of 0.5

temperature is much lower as compared to the other two cases. In the first two scenarios, only the scaling parameter is uncertain, whereas in the third example we consider only directional uncertainty. We know that under the assumption of deterministic boundary conditions, the random temperature field $T(x, \omega)$ varies inversely to the stochastic coefficient $\kappa_r(\omega_r)$. As the scaling parameters of the model $\kappa_r(\omega_r)$ remain constant, the impact on the variation of temperature field $T(x, \omega)$ due to directional randomness is small. On the other hand, when the scaling parameters are modelled as varying, the standard deviation estimate of temperature $T_{h,N}$ becomes more sensitive as evident in Figs. 6(a) and 6(b). Interestingly, when Fig. 6(b) is compared to Fig. 6(a), it is clear that, varying the material symmetry from higher (isotropy) to lower (orthotropy) order in the model iso-ortho-scl results in lower stochastic influence on temperature $T_{h,N}$.

Furthermore, the sample mean estimates of total heat flux (THFL) $q_{h,N}^{(t)}$ are presented in Fig. 7, where, Figs. 7(a) and 7(b) showcase similar results as described previously (see Figs. 5(a) and 5(b)). However, in comparison to these two figures, a visible difference in maximum total heat flux and contour pattern is noticed in Fig. 7(c). In Fig. 8, the corresponding estimated standard deviation of THFL $q_{h,N}^{(t)}$ is plotted. Here, the most interesting aspect is seen in Fig. 8(a), where, the standard deviation is close to zero. It turns out that, in the model iso-iso-scl, the stochastic coefficient $\kappa_s(\omega_s)$ has almost perfect inverse correlation with temperature gradient field $\nabla T(\mathbf{x}, \omega)$. Thus, the randomness in the model $\kappa_s(\omega_s)$ has almost no stochastic impact on THFL $q_{h,N}^{(t)}$. However, on the contrary, the estimate in Figs. 8(b) and 8(c) is visible, signifying the stochastic influence of the

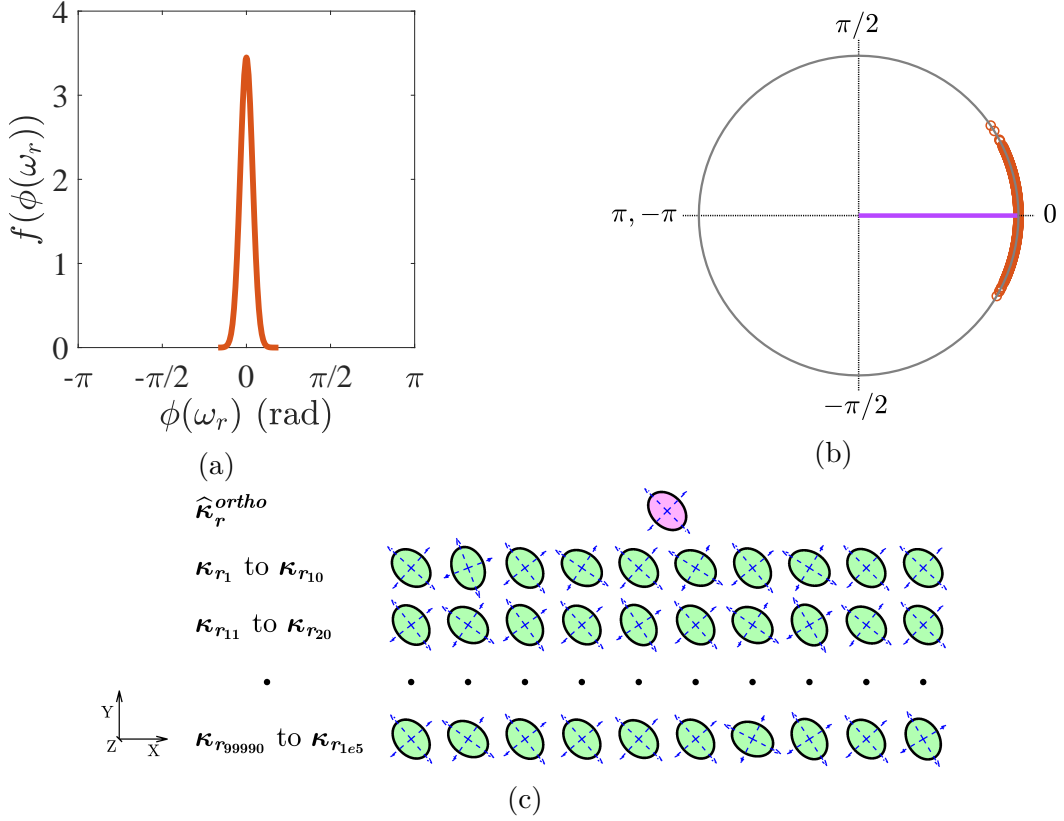


Figure 4: Stochastic tensor $\kappa_r(\omega_r)$ with fixed symmetry (ortho-ortho-dir): (a) von Mises PDF of random rotation angle $\phi(\omega_r)$, (b) realisations of circular random variable $\phi(\omega_r)$ on unit circle with resultant mean vector (solid straight line), (c) geometric visualization of reference tensor $\hat{\kappa}_r^{ortho}$ and realisations of random tensor $\kappa_r(\omega_r)$; the geometries are enhanced by scaling the eigenvalues by a factor of 0.5, and the orientations with respect to the mean are scaled by a factor of 1.5

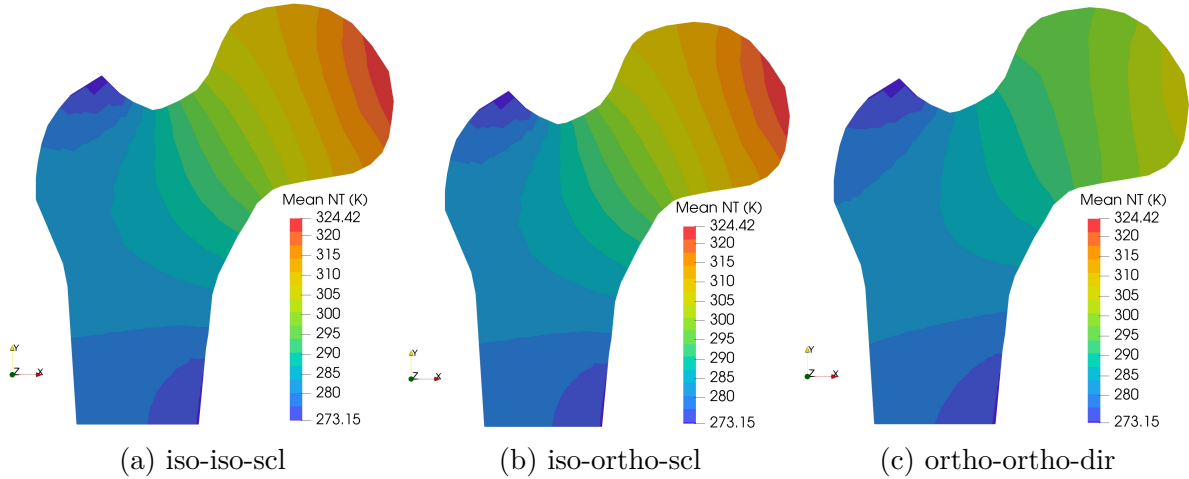


Figure 5: MC mean estimate of nodal temperature

considered input models on THFL $q_{h,N}^{(t)}$. One may conclude that directivity has more impact on the heat flux than the scaling parameter.

Furthermore, the directional mean $\mu_{\text{circ}}^{(\text{MC})}(\hat{q}_{h,N})$ and standard deviation $\text{Std}_{\text{circ}}^{(\text{MC})}(\hat{q}_{h,N})$ of normalized heat flux (NHFL) $\hat{q}_{h,N}$ —from Eqs. (34) and (35)—are displayed in Fig. 9.

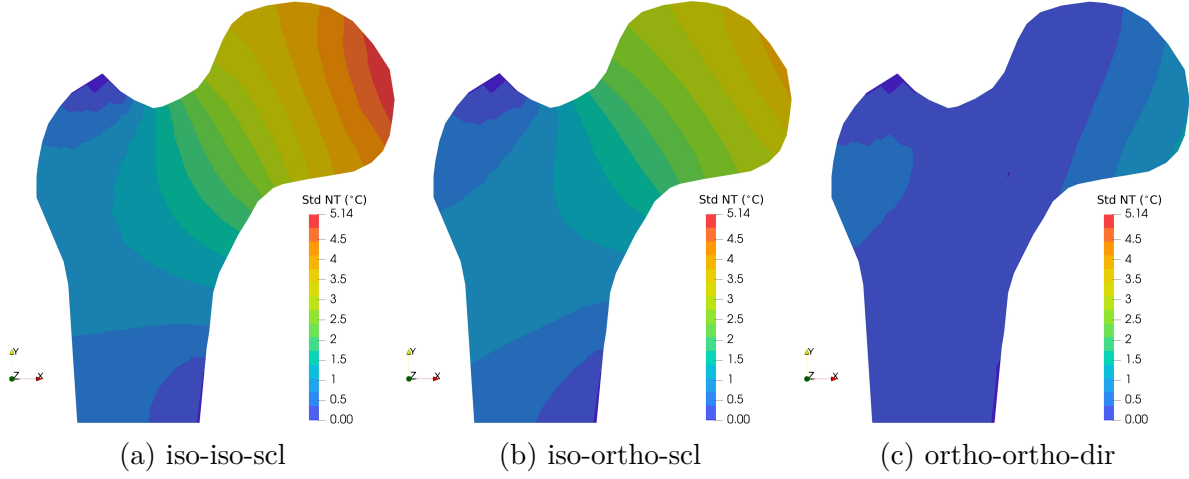


Figure 6: MC standard deviation estimate of nodal temperature

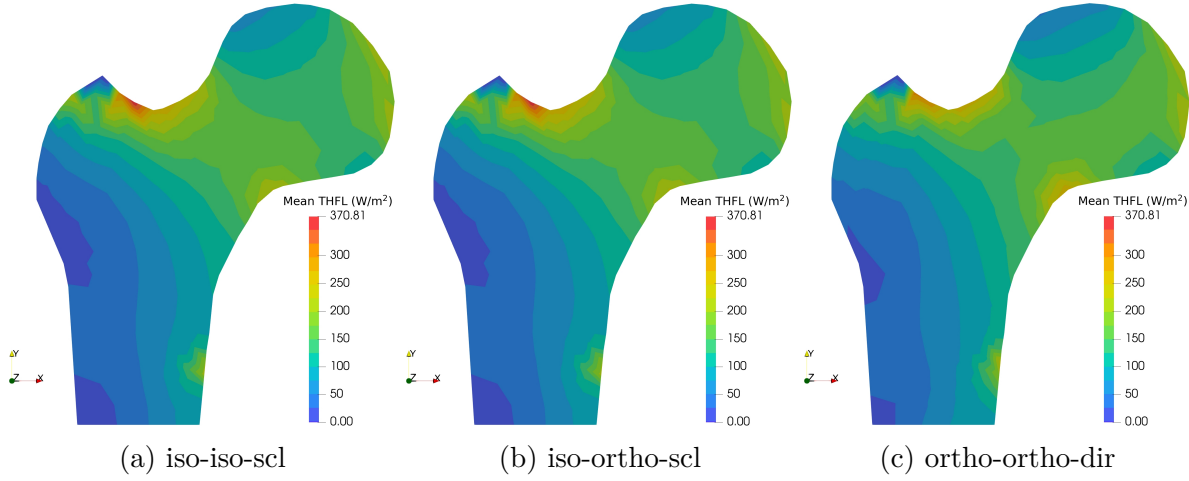


Figure 7: MC mean estimate of total heat flux (Euclidean norm)

The mean orientation (vector representation) in Figs. 9(a) and 9(b) look similar, however, with a closer inspection of Fig. 9(c), the difference is apparent. Similar to the results in Fig. 8, the circular standard deviation estimate in Fig. 9(a) is also close to zero, showing once again the insensitivity of directional attribute of NHFL $\hat{\mathbf{q}}_{h,N}$ to scaling uncertainty present in the model $\kappa_s(\omega_s)$. Also, in comparison, the standard deviation estimate in Fig. 9(c) is more significant than in Fig. 9(b).

6. Results on 3D proximal femur

A three-dimensional proximal femur configuration of dimensions 45mm in width and 154mm in height is considered. The boundary conditions with identical values as used in the 2D example are imposed, shown in Fig. 10. The computational domain is discretized by a four-noded tetrahedral finite element mesh, comprising 12504 nodes, 3166 elements and 35115 degrees of freedom. We use similar modelling scenarios as in 2D case i.e. iso-iso-scl, iso-ortho-scl and ortho-ortho-dir (see Table 2 for model abbreviations). The considered isotropic $\hat{\kappa}_s^{iso} \in \text{Sym}^+(3)$ and orthotropic $\hat{\kappa}_r^{ortho} \in \text{Sym}^+(3)$ reference conductivity tensors are tabulated in Table 4. Furthermore, by fixing negative y-axis as the rotational axis, the directional vectors of the model $\hat{\kappa}_r^{ortho}$ corresponding to the eigenvalues $\hat{\lambda}_r^{(1)}$ and $\hat{\lambda}_r^{(3)}$

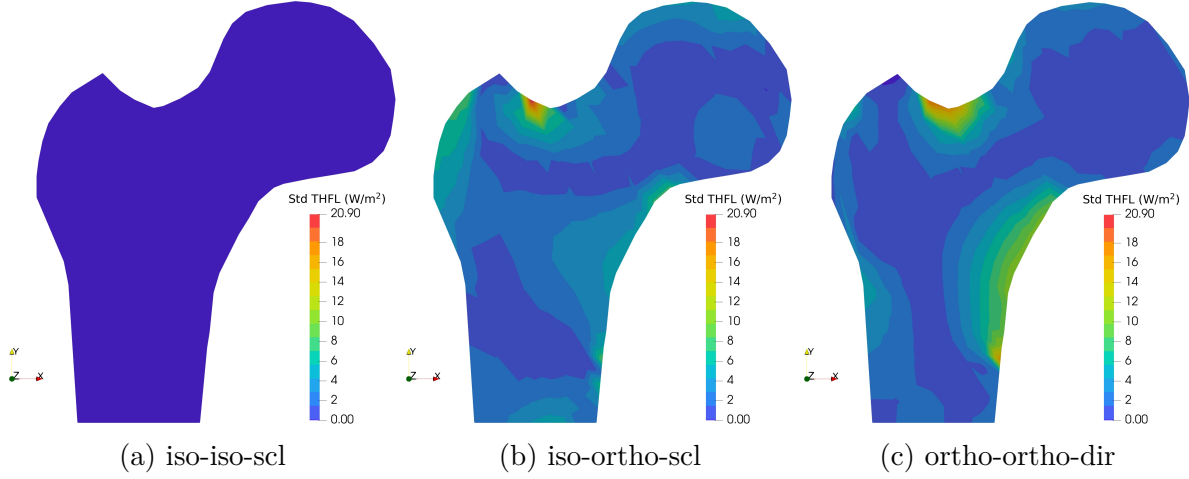


Figure 8: MC standard deviation estimate of total heat flux (Euclidean norm)

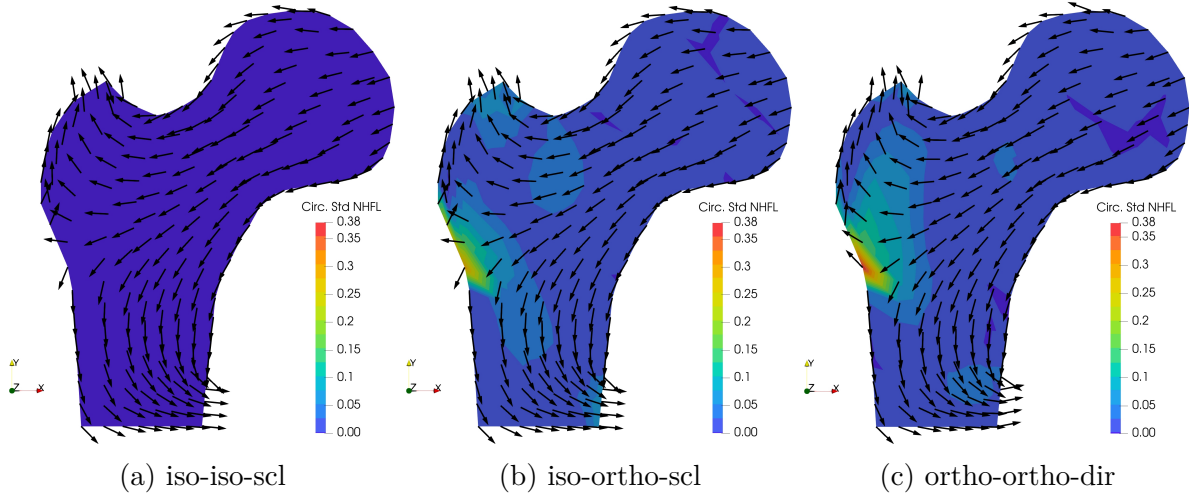


Figure 9: MC circular mean (vector representation) and circular standard deviation estimates (dimensionless quantity) of normalized heat flux

are positioned at an angle of $\pi/4$ in an anti-clockwise direction with respect to x and z-axis, respectively.

Random scaling with fixed symmetry: a stochastic tensor $\kappa_s(\omega_s) \in \text{Sym}^+(3)$ with fixed symmetry (iso-iso-scl), where the random scaling elements $\lambda_s^{(1)}(\omega_s) = \lambda_s^{(2)}(\omega_s) = \lambda_s^{(3)}(\omega_s)$ are modelled by the identical and dependent log-normal random variables, is constructed (see Eq. (14) for the exponential mapping). The schematic representation of the model is shown in Fig. 11, where Fig. 11(a) presents the log-normal PDF of scaling parameters $\{\lambda_s^{(i)}(\omega_s)\}_{i=1}^3$, whereas the geometric visualization—in the form of equivalent spheres—of the reference tensor $\hat{\kappa}_s^{iso}$ and realisations $\{\kappa_{s_i}\}_{i=1}^N$ is displayed in Fig. 11(b). Here the radius of the sphere is determined by $1/\sqrt{\lambda_s^{(1)}(\omega_s)}$, $1/\sqrt{\lambda_s^{(2)}(\omega_s)}$ and $1/\sqrt{\lambda_s^{(3)}(\omega_s)}$. As can be seen that the radius of the spheres in the realisations vary and the spherical shape of the mean is maintained in the realisations, owing to the preservation of isotropic material symmetry in the mean and realisations.

Random scaling with varying symmetry: a random tensor model $\kappa_s(\omega_s) \in \text{Sym}^+(3)$ similar to the previous scenario, however with a varying material symmetry (iso-ortho-scl) is showcased in Fig. 12. In Fig. 12(a), the PDF of i.i.d log-normal scaling

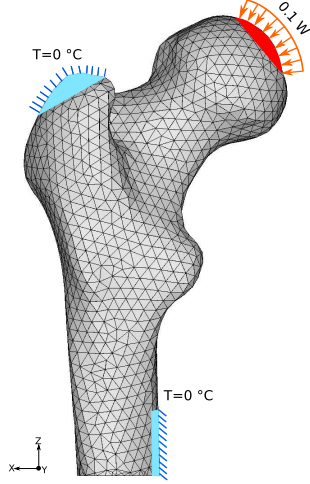


Figure 10: Boundary conditions of 3D femur bone

isotropy [W/m·K] $\hat{\kappa}_s^{iso}$	orthotropy [W/m·K] $\hat{\kappa}_r^{ortho}$
$\begin{bmatrix} 0.54 & 0 & 0 \\ 0 & 0.54 & 0 \\ 0 & 0 & 0.54 \end{bmatrix}$	$\begin{bmatrix} 0.77 & 0 & 0.23 \\ 0 & 0.75 & 0 \\ 0.23 & 0 & 0.77 \end{bmatrix}$
Eigenvalues [W/m·K]	
$\hat{\lambda}_s^{(1)} = 0.54, \hat{\lambda}_s^{(2)} = 0.54$ $\hat{\lambda}_s^{(3)} = 0.54$	$\hat{\lambda}_r^{(1)} = 0.54, \hat{\lambda}_r^{(2)} = 0.75$ $\hat{\lambda}_r^{(3)} = 1$

Table 4: Reference conductivity tensors with corresponding eigenvalues of 3D femur

parameters $\{\lambda_s^{(i)}(\omega_s)\}_{i=1}^3$ can be seen, whereas Fig. 12(b) shows the geometric interpretation of the mean $\hat{\kappa}_s^{iso}$ and realisations $\{\kappa_{si}\}_{i=1}^N$. Looking from the negative y-axis, the eigenvectors of the model $\kappa_s(\omega_s)$ conforming to the eigenvalues $\hat{\lambda}_s^{(1)}$ and $\hat{\lambda}_s^{(3)}$ are at an angle of $\pi/4$ in an anti-clockwise direction corresponding to x and z-axis, respectively. A change in symmetry from isotropic in the mean (spherical shape) to orthotropic (ellipsoidal shape) in the realisations is evident. Also, the fluctuation in lengths of semi-major axes—calculated by $1/\sqrt{\lambda_s^{(1)}(\omega_s)}$, $1/\sqrt{\lambda_s^{(2)}(\omega_s)}$ and $1/\sqrt{\lambda_s^{(3)}(\omega_s)}$ —of the ellipsoids represents the aspect of varying scaling parameters.

Random orientation with fixed symmetry: to account for directional uncertainty only, a random tensor with fixed symmetry (ortho-ortho-dir) $\kappa_r(\omega_r) \in \text{Sym}^+(3)$, which is the exponential of the model described in Eq. (17), is considered. The unit axis vector $\mathbf{v}(\omega_r)$ is modelled as a von Mises-Fisher distribution (see Eq. (29)) with the mean direction $\boldsymbol{\mu}_{\text{circ}}$ (the eigenvector of the reference tensor $\hat{\kappa}_r^{ortho}$ which corresponds to the eigenvalue $\hat{\lambda}_r^{(3)}$), and the concentration parameter $\eta = 75$. The random rotational angle $\phi(\omega_r)$ is then determined using the dot product operation, $\phi(\omega_r) = \arccos(\boldsymbol{\mu}_{\text{circ}} \cdot \mathbf{v}(\omega_r))$. Following this, the corresponding random rotation matrix $\mathbf{R}(\omega_r)$ is constructed as per the Rodrigues rotation formula described in Eq. (20). Fig. 13 summarizes the model $\kappa_r(\omega_r)$, where Fig. 13(a) displays the mean and realisations of von Mises Fisher random variable on unit sphere, and the equivalent ellipsoidal representation of stochastic model $\kappa_r(\omega_r)$ is

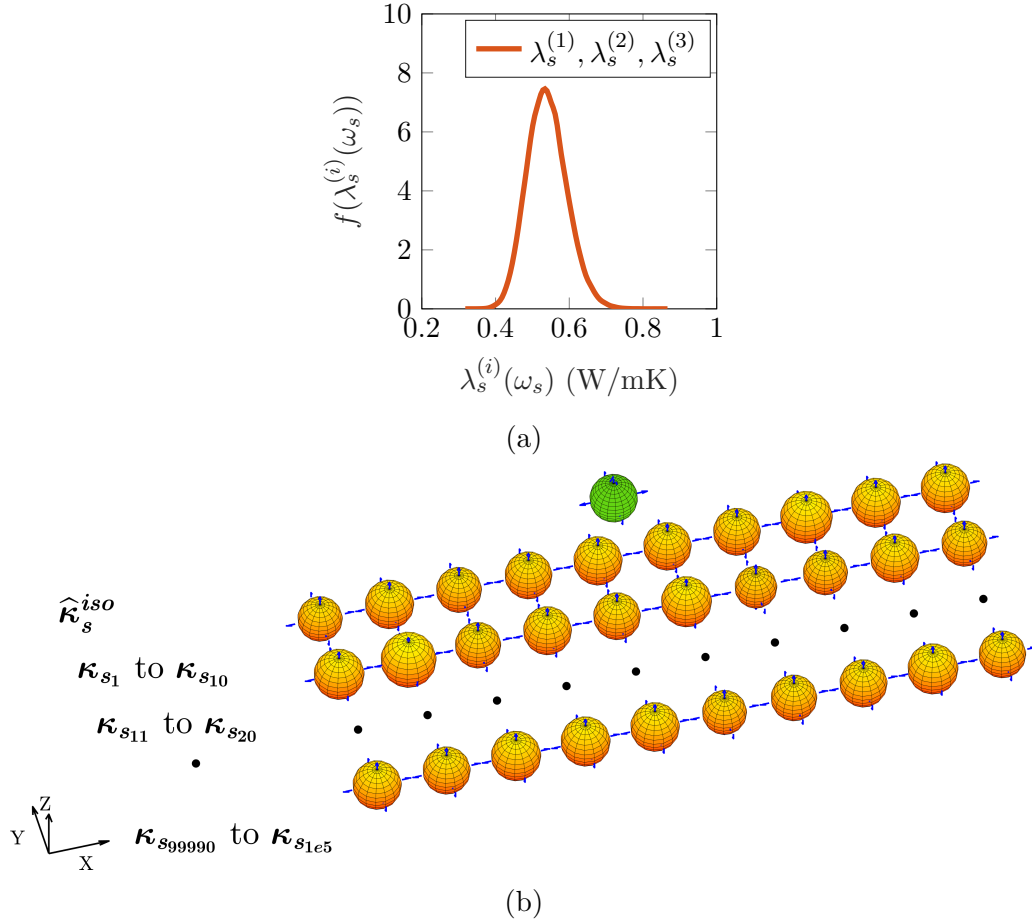


Figure 11: Stochastic tensor $\kappa_s(\omega_s)$ with fixed symmetry (iso-iso-scl): (a) log-normal PDF of identical and dependent random scaling values $\lambda_s^{(1)}(\omega_s) = \lambda_s^{(2)}(\omega_s) = \lambda_s^{(3)}(\omega_s)$, (b) geometric visualization of reference tensor $\hat{\kappa}_s^{iso}$ and realisations of random tensor $\kappa_s(\omega_s)$; the geometries are enhanced by scaling the eigenvalues by a factor of 0.5

portrayed in Fig. 13(b). It is evident that the shape and size of the ellipsoid in the mean and realisations remain constant; only the orientation of semi-axes of ellipsoids in the realisations fluctuate.

Uncertainty quantification: Figs. 14-17 display the MC mean and standard deviation estimates of NT and THFL, whereas Fig. 18 shows the circular MC mean and circular standard deviation estimate of NHFL. Concerning the sensitivity of different stochastic models on the desired quantities, we make similar observations, and hence, draw similar conclusions on the 3D example as in the previous 2D case (from Section 5). That is, the findings in Figs. 5-9 correspond approximately to the results in Figs. 14-18.

The numerical results of both 2D and 3D proximal femur signify the prominence of incorporating different material uncertainties—scaling, orientation and material symmetry—independently into the constitutive model; the results showcase the distinct impact of stochastic models on the desired quantities of interest, such as nodal temperature and heat flux.

7. Conclusion

Here the task of modelling and representing random symmetric and positive definite (SPD) tensors was addressed, and some desiderata for the modelling and representation

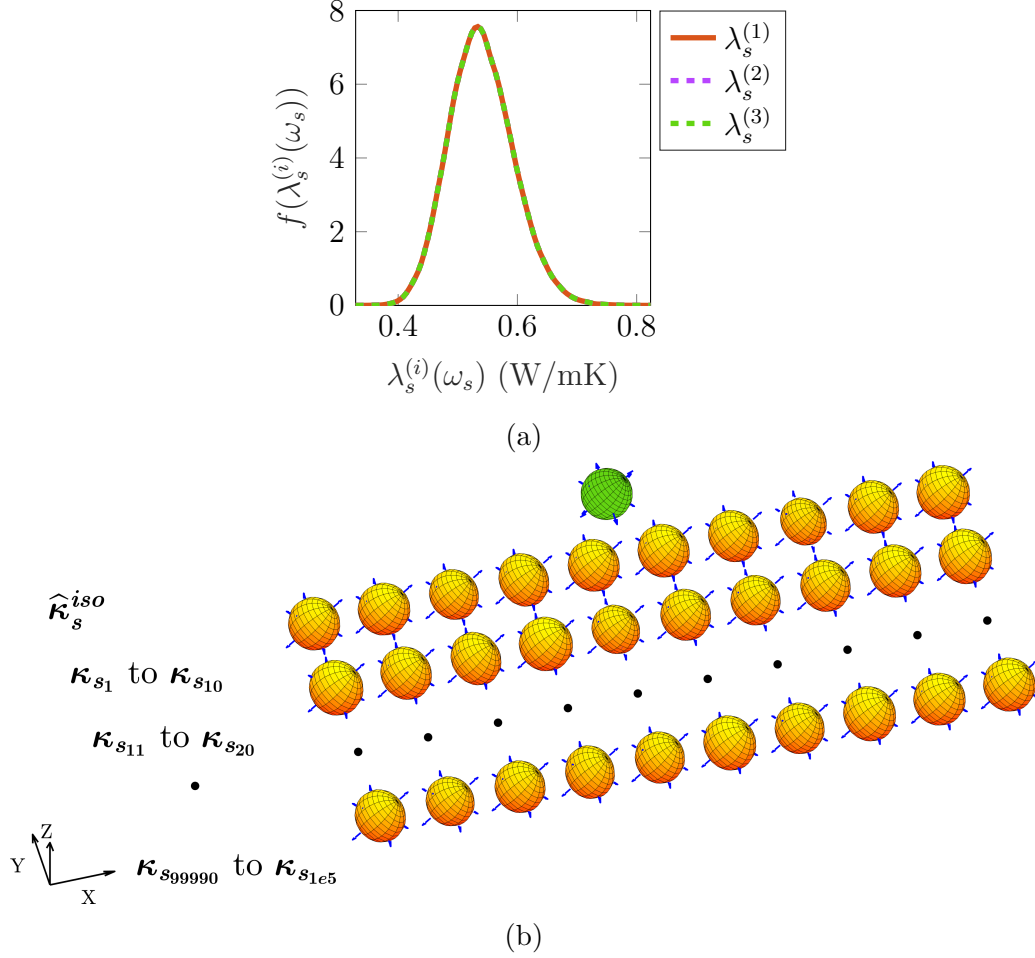


Figure 12: Stochastic tensor $\kappa_s(\omega_s)$ with varying symmetry (iso-ortho-scl): (a) log-normal PDF of i.i.d random scaling values $\{\lambda_s^{(i)}(\omega_s)\}_{i=1}^3$, (b) geometric visualization of reference tensor $\hat{\kappa}_s^{iso}$ and realisations of random tensor $\kappa_s(\omega_s)$; the geometries are enhanced by scaling the eigenvalues by a factor of 0.5

were formulated. Namely, the representation has to be SPD even under numerical approximation, and has to be such that one is able to control the material or spatial invariance resp. symmetry, both for each possible realisation and for the the expected value. Regarding the mean or expected value, it turned out that the usual expectation, which is tied to the structure of a linear space, may not be appropriate on the open convex cone of SPD tensors. The more general Fréchet mean is based on distance measurements, possibly different from the usual Euclidean distance, on the set of SPD tensors. Here some desiderata were formulated for the distance measure, which take into account the physical purpose and uncertainty involved in stochastic models of such physically symmetric and positive definite tensors.

Therefore in [Appendix A](#) the type of metric that one can consider for symmetric positive tensors and specifically for the set of SPD matrices to compute the corresponding Fréchet mean is discussed. As the Euclidean mean suffers from the so-called swelling effect, we suggest alternatives such as the geometric, log-Euclidean, and scale-rotation separated mean. The inappropriateness of the Euclidean mean for random SPD matrices with random orientation in a 2D case is further explored in more detail in [Appendix B](#).

It was also proposed to follow a widely used technique and to model and represent the

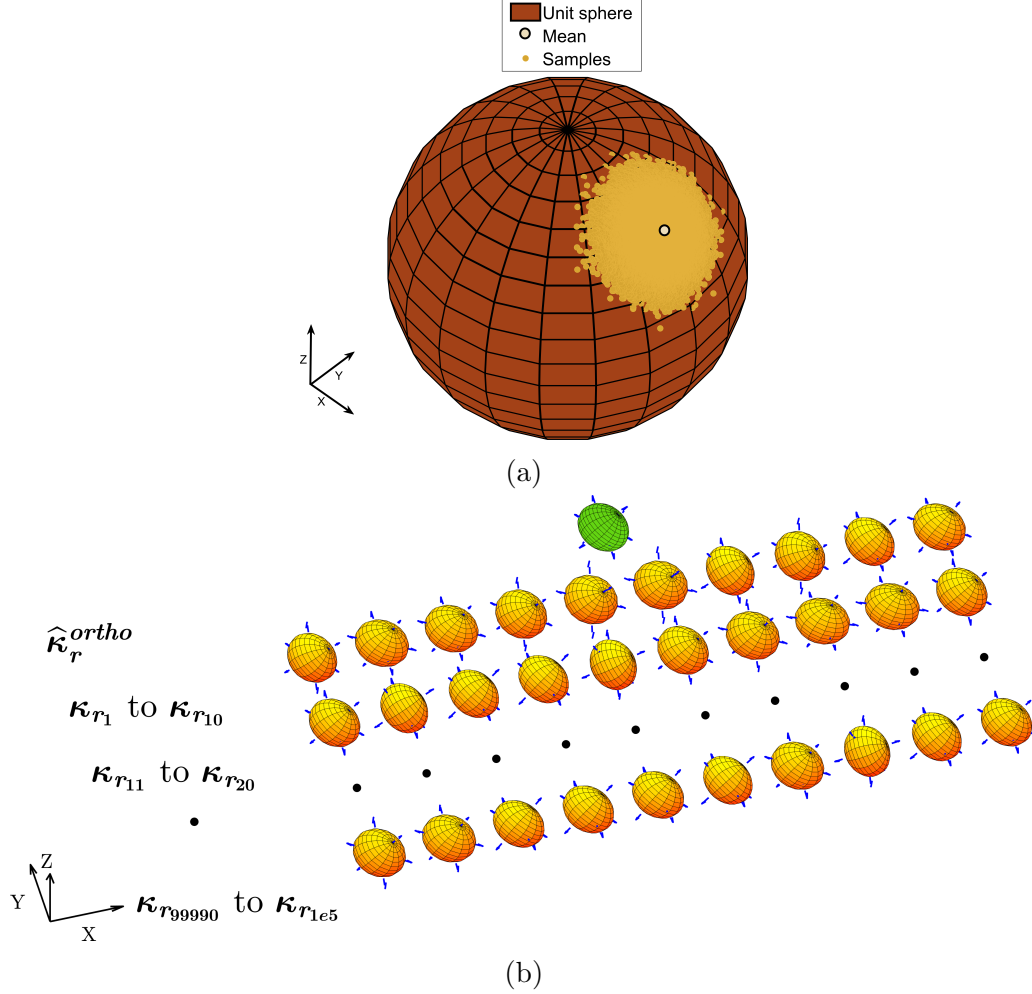


Figure 13: Stochastic tensor $\kappa_r(\omega_r)$ with fixed symmetry (ortho-ortho-dir): (a) realisations of von Mises Fisher random variable $\mathbf{v}(\omega_r)$ on unit sphere with mean $\boldsymbol{\mu}_{\text{circ}}$, (b) geometric visualization of reference tensor $\hat{\kappa}_r^{\text{ortho}}$ and realisations of random tensor $\kappa_r(\omega_r)$; the geometries are enhanced by scaling the eigenvalues by a factor of 0.5, and the orientations with respect to the mean are scaled by a factor of 1.5

logarithm of tensor, such that the symmetric positive definite attribute is automatically satisfied when taking the exponential in the end; the invariance properties automatically translate to the logarithm. To expose the ideas in the simplest possible setting, we consider specifically second-order SPD tensors, and only fields spatially constant with each realisation, i.e. SPD tensor-valued random variables.

More particularly, the focus is on modelling uncertainties in such a way as to have a fine control independently over the strength/scaling and directional attributes of the tensor—given that the material symmetry is fixed. As we separate the strength and orientation of the random SPD matrices by spectral decomposition, the task boils down to modelling the random scaling parameters of the logarithm of a random diagonal matrix, as well as the random orthogonal matrix of eigenvectors. Such orthogonal matrices are members of the Lie group $\text{SO}(d)$, and the well-known exponential map from the corresponding Lie algebra $\mathfrak{so}(d)$ of skew-symmetric matrices was used to carry random ensembles in the free vector space $\mathfrak{so}(d)$ onto such ensembles on $\text{SO}(d)$. This results in the random orientation being modelled by symmetric circular/spherical distributions. Furthermore, a scenario of

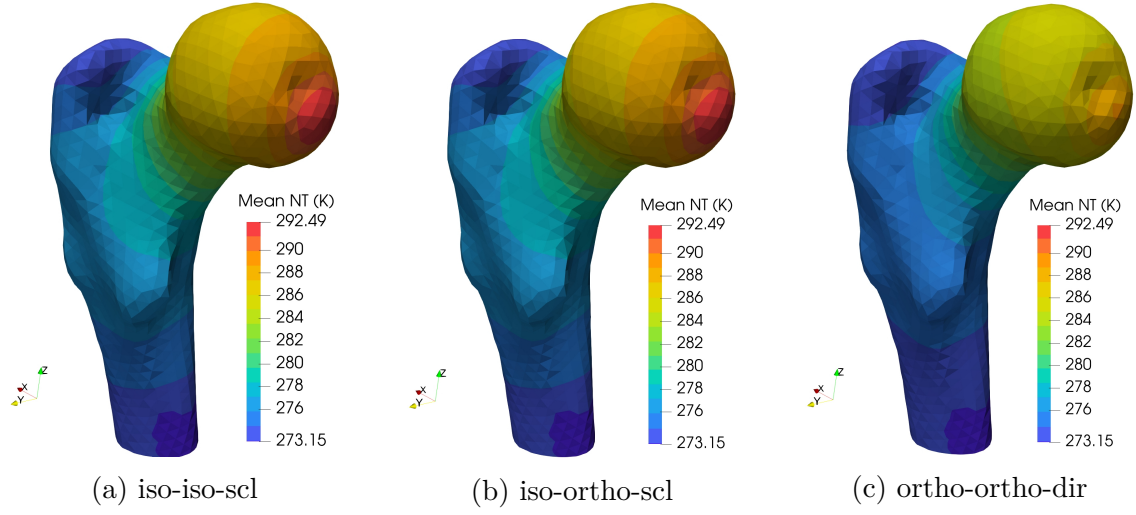


Figure 14: MC mean estimate of nodal temperature

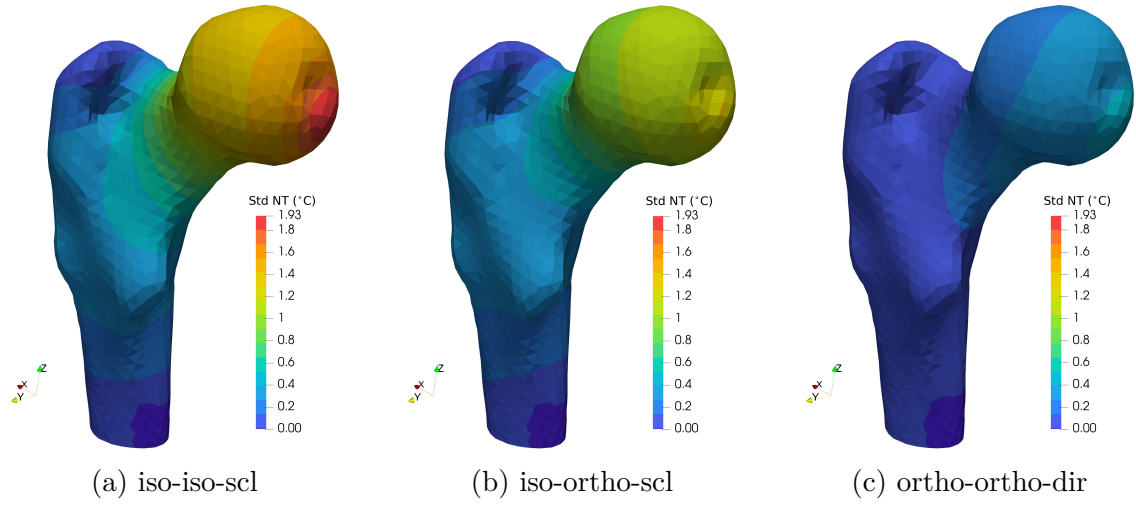


Figure 15: MC standard deviation estimate of nodal temperature

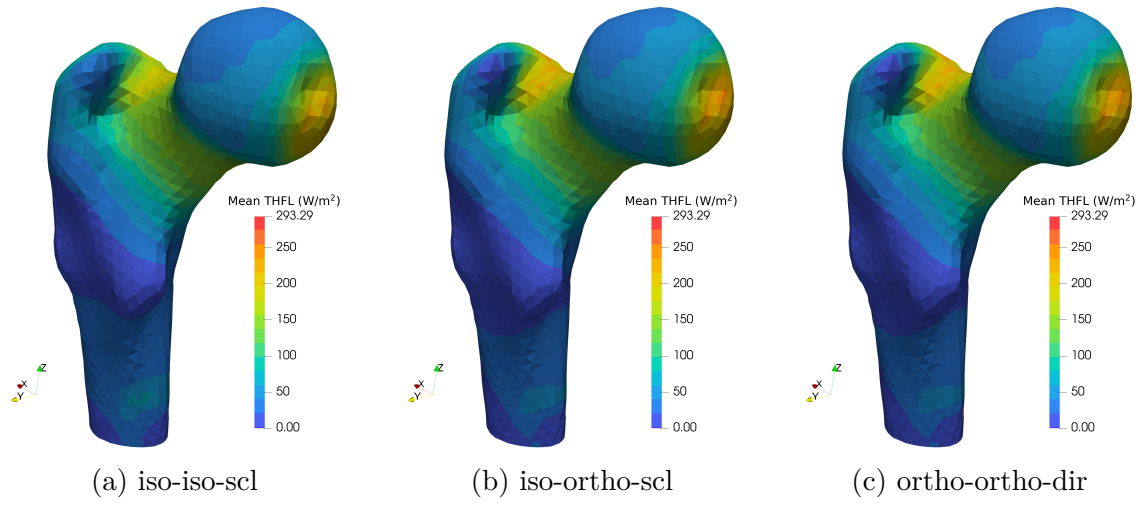


Figure 16: MC mean estimate of total heat flux (Euclidean norm)

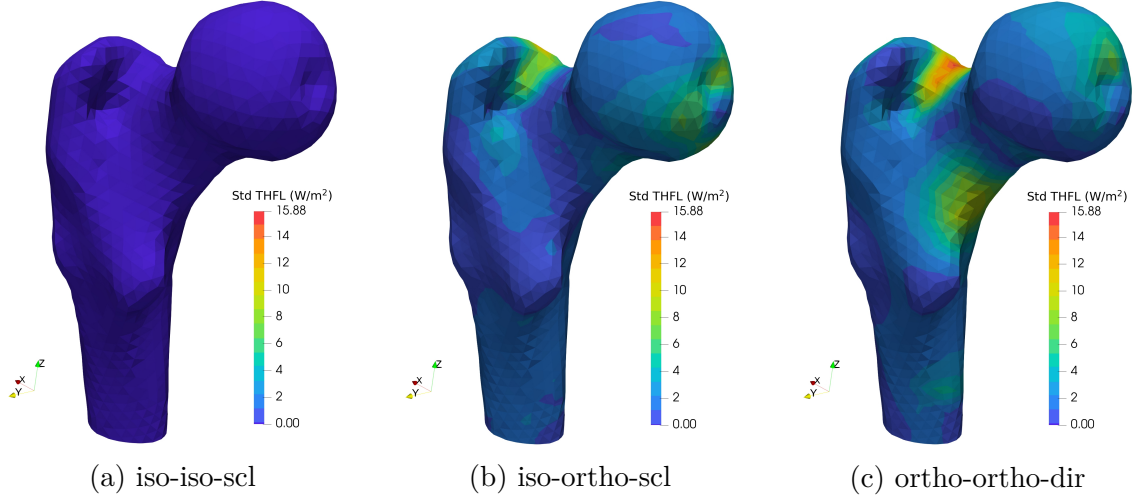


Figure 17: MC standard deviation estimate of total heat flux (Euclidean norm)

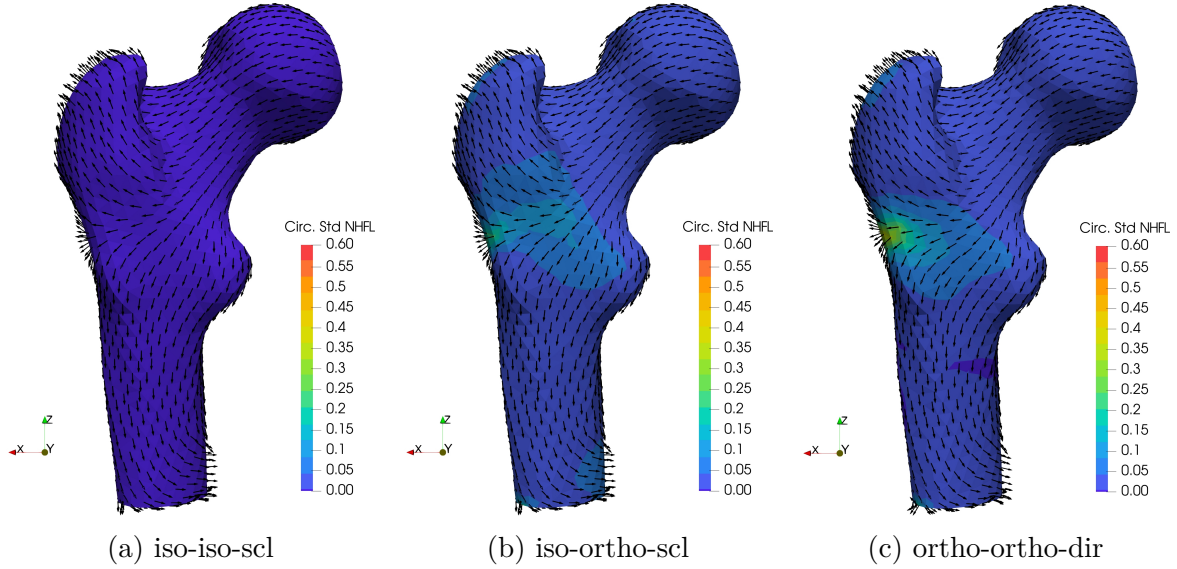


Figure 18: MC circular mean (vector representation) and circular standard deviation estimates (dimensionless quantity) of normalized heat flux

fluctuating the material symmetry around the Fréchet mean is also studied, i.e. the mean tensor belongs to a higher order of material or spatial symmetry, whereas each realisation belongs to a lower order of material symmetry.

As an application in this study, we model the random thermal conductivity tensor of a steady-state heat conduction on a 2D and a 3D model of a proximal femur bone, a highly anisotropic material. Three different modelling scenarios are investigated: random scaling only, random scaling with fluctuating symmetry, and random orientation only. The material uncertainties are then propagated to the output responses such as nodal temperature (NT), total heat flux (THFL) and normalized heat flux (NHFL) using the Monte Carlo method (MC). Subsequently, statistics such as mean and standard deviation estimates of NT and THFL, and circular mean and circular standard deviation estimates of NHFL are determined.

From the numerical results of both 2D and 3D models, it is clear that NT is most stochastically sensitive to the model with random scaling only, and least sensitive to

random orientation only. On the other hand, the randomness in the model with random scaling only has almost zero stochastic influence on THFL—determined by the Euclidean norm—but the impact of the other two random models is evident. We also see a similar stochastic sensitivity of the stochastic models on NHFL, as well as on THFL. Therefore, the distinctive impact of the three stochastic models on the output response signifies the importance of incorporating different material uncertainties—scaling, orientation and material symmetry—independently into the constitutive model.

In total, we have proposed a modelling scenario for tensors defining positive-definite material properties which takes into account possible material resp. spatial invariances or symmetries. Our approach allows a fine control of the scaling randomness, and independently of the orientation randomness, further separating it into the invariance properties of the mean and those of the random fluctuations.

Appendix A. Metrics on symmetric positive definite matrices

What metric to take instead of the Euclidean one connected with the arithmetic mean is not so clear. Various options are explored e.g. in [36], see also the discussion in [16]. The open convex cone $\text{Sym}^+(d) \subset \text{Sym}(d)$ may be considered as a metric space in ways different from just being a subset of the vector space $\text{Sym}(d)$. In addition to the desiderata listed in Section 2 for a metric, one may want that $\vartheta_D(\mathbf{I}, \alpha \mathbf{C}) \rightarrow \infty$ as $\alpha \rightarrow \infty$ for any $\mathbf{C} \in \text{Sym}^+(d)$, but the same should also hold as $\alpha \rightarrow 0$, in fact singular matrices in $\text{Sym}(d)$ should all be infinitely far away from the identity, i.e. all of the boundary $\partial \text{Sym}^+(d) \subset \text{Sym}(d)$ should be at an infinite distance from the identity.

As an open convex cone in a Euclidean space, $\text{Sym}^+(d)$ can be considered as a Riemannian manifold with tangent space $\text{Sym}(d)$ with the Euclidean inner product at each point. This gives a metric ϑ_G on $\text{Sym}^+(d)$ which leads to the so-called geometric or affine-invariant mean [1, 35, 36] $\vartheta_G(\mathbf{C}_1, \mathbf{C}_2) := \|\log(\mathbf{C}_1^{-1/2} \mathbf{C}_2 \mathbf{C}_1^{-1/2})\|_F$. Observe that $\mathbf{C}_1^{-1/2} \mathbf{C}_2 \mathbf{C}_1^{-1/2} \in \text{Sym}^+(d)$, and the existence of a unique logarithm is guaranteed by the spectral calculus [41, 43]. One may remark that $\vartheta_G(\mathbf{C}_1, \mathbf{C}_2) = \sum_k (\log \lambda_k)^2$, where λ_k are the eigenvalues of the matrix pencil $(\mathbf{C}_1, \mathbf{C}_2)$, i.e. the eigenvalues of the generalised eigenvalue problem $\mathbf{C}_1 \mathbf{s}_k = \lambda_k \mathbf{C}_2 \mathbf{s}_k$. This distance satisfies all the desired properties [1, 35, 36] listed in Section 2, as well as that the boundary $\partial \text{Sym}^+(d)$ is infinitely far away from the identity—this is here a consequence of working with $\log \mathbf{C}$. But other choices for the metric are possible [15, 16]. Observe that when \mathbf{C}_1 and \mathbf{C}_2 commute, $\vartheta_G(\mathbf{C}_1, \mathbf{C}_2) = \|\log \mathbf{C}_2 - \log \mathbf{C}_1\|_F$, and many of the problems of defining a suitable metric are connected with the difficulties arising from non-commuting tensors.

One may recall that for a connected compact Lie group like the special orthogonal group $\text{SO}(d)$ which is used in our approach, one may define a metric invariant under the action of the group on itself (e.g. [34]), which is hence a very natural way to obtain a metric. It takes advantage of the correspondence between the Lie group $\text{SO}(d)$ and its Lie algebra $\mathfrak{so}(d)$ of skew-symmetric matrices given by the exponential map resp. the logarithm, and is given by $\vartheta_R(\mathbf{Q}_1, \mathbf{Q}_2) := \|\log(\mathbf{Q}_1^T \mathbf{Q}_2)\|_F$ for $\mathbf{Q}_1, \mathbf{Q}_2 \in \text{SO}(d)$. Observe that $\mathbf{Q}_1^T \mathbf{Q}_2 \in \text{SO}(d)$ and hence $\log(\mathbf{Q}_1^T \mathbf{Q}_2) \in \mathfrak{so}(d)$, and if \mathbf{Q}_1 and \mathbf{Q}_2 commute, $\log(\mathbf{Q}_1^T \mathbf{Q}_2) = \log \mathbf{Q}_2 - \log \mathbf{Q}_1$; compare this with ϑ_G above in the commutative case. In any case, straight lines in the Lie algebra of skew matrices $\mathfrak{so}(d)$ are geodesics with the Frobenius distance, and these are mapped by the exponential map—the inverse of the logarithm—onto geodesics in $\text{SO}(d)$. It may be also noted that the exponential map and its inverse, the logarithm, establish a correspondence between the Lie algebra $\mathfrak{so}(d)$ —which is one-to-one in the ball

of $\mathbf{W} \in \mathfrak{so}(d)$ defined as in Eq. (19) by Euler-vectors in the ball $\{\mathbf{w} \in \mathbb{R}^3 \mid \|\mathbf{w}\| \leq \pi\}$ with antipodal points identified—and the Lie group $\text{SO}(d)$, see also [6].

Unfortunately, when considering these results for Lie groups, one has to note that $\text{Sym}^+(d)$ is not a group under matrix multiplication, although—as was already noted—it is stable or invariant under inversion. But taking the situation for $\text{SO}(d)$ as a cue, it has been found [3] that there is a way of making $\text{Sym}^+(d)$ into a Lie group with a new and commutative definition of multiplication:

$$\forall \mathbf{C}_1, \mathbf{C}_2 \in \text{Sym}^+(d) : \mathbf{C}_1 \boxtimes \mathbf{C}_2 := \exp(\log \mathbf{C}_1 + \log \mathbf{C}_2). \quad (\text{A.1})$$

This makes $\text{Sym}^+(d)$ into a commutative Lie group [3] with the multiplication ‘ \boxtimes ’—indeed, the inverse of $\mathbf{C} \in \text{Sym}^+(d)$ w.r.t. this multiplication is the normal matrix inverse $\mathbf{C}^{-1} \in \text{Sym}^+(d)$, and the neutral element is the normal identity matrix $\mathbf{I} \in \text{Sym}^+(d)$ —and whenever \mathbf{C}_1 and \mathbf{C}_2 commute, this new product indeed coincides with the normal matrix product. Further it can be shown [3] that the Lie algebra of this Lie Group $(\text{Sym}^+(d), \boxtimes)$ is the vector space of symmetric matrices $\text{Sym}(d)$, and the exponential map in the sense of Lie algebras is indeed the matrix exponential. In fact, the exponential map and its inverse, the logarithm, establish a one-to-one correspondence between the Lie algebra $\text{Sym}(d)$ and the Lie group $\text{Sym}^+(d)$, actually a diffeomorphism and an algebraic isomorphism between the groups $(\text{Sym}^+(d), \boxtimes)$ (with the new multiplication) and the additive group $(\text{Sym}(d), +)$ of the vector space of symmetric matrices. This means in particular that straight lines—geodesics with the Euclidean or Frobenius distance in $\text{Sym}(d)$ —are mapped into geodesics in $\text{Sym}^+(d)$ with the logarithmic or log-Euclidean metric $\vartheta_L(\mathbf{C}_1, \mathbf{C}_2) := \|\log \mathbf{C}_1 - \log \mathbf{C}_2\|_F$, which also satisfies all desiderata listed in Section 2, and has the boundary $\partial \text{Sym}^+(d)$ at an infinite distance from the identity. Among others, this metric is also investigated in [15] (the authors call ϑ_L the *chaotic geometric distance*) and [40]. Notice also the equality with ϑ_G above for the commuting case—if \mathbf{C}_1 and \mathbf{C}_2 commute, $\vartheta_L(\mathbf{C}_1, \mathbf{C}_2) = \|\log(\mathbf{C}_1 \mathbf{C}_2^{-1})\|_F = \vartheta_G(\mathbf{C}_1, \mathbf{C}_2)$ —and also the similarity with the Riemannian metric ϑ_R on $\text{SO}(d)$. This means that the two metrics ϑ_G and ϑ_L agree on commuting subsets of $\text{Sym}^+(d)$.

Another possibility arises from the observation that two tensors $\mathbf{C}_1, \mathbf{C}_2 \in \text{Sym}^+(d)$ commute only if they have the same invariant subspaces. In that case it can be arranged that the eigenvector matrices according to the spectral decomposition Eq. (9), $\mathbf{C}_1 = \mathbf{Q}_1 \mathbf{\Lambda}_1 \mathbf{Q}_1^T$ and $\mathbf{C}_2 = \mathbf{Q}_2 \mathbf{\Lambda}_2 \mathbf{Q}_2^T$, are equal, i.e. $\mathbf{Q}_1 = \mathbf{Q}_2$. In this instance of two commuting tensors, one has

$$\begin{aligned} \vartheta_L(\mathbf{C}_1, \mathbf{C}_2) &= \vartheta_G(\mathbf{C}_1, \mathbf{C}_2) \\ &= \vartheta_L(\mathbf{\Lambda}_1, \mathbf{\Lambda}_2) = \|\log \mathbf{\Lambda}_1 - \log \mathbf{\Lambda}_2\|_F = \|\log(\mathbf{\Lambda}_1 \mathbf{\Lambda}_2^{-1})\| = \sqrt{\sum_k (\log(\lambda_{k,1}/\lambda_{k,2}))^2}. \end{aligned}$$

From this one may come to the idea [24, 16] to measure the distance on $\text{Sym}^+(d)$ by measuring separately the distance between the eigenspaces (rotation) and the distance between the eigenvalues (scaling), and one may define a distance function (not always a metric [16]) $\vartheta_S(\mathbf{C}_1, \mathbf{C}_2)^2 = \vartheta_L(\mathbf{\Lambda}_1, \mathbf{\Lambda}_2)^2 + c \vartheta_R(\mathbf{Q}_1, \mathbf{Q}_2)^2$ for some $c > 0$, i.e. measure the distance between the scales and the orientations separately and add them both up. It is not difficult to see that ϑ_S also satisfies all our desiderata listed in Section 2, and the boundary $\partial \text{Sym}^+(d)$ is infinitely far away from the identity.

As we propose to rather work with $\mathbf{H} = \log(\mathbf{C}) \in \text{Sym}(d)$, where $\log(\mathbf{Q} \mathbf{\Lambda} \mathbf{Q}^T) = \mathbf{Q} \log(\mathbf{\Lambda}) \mathbf{Q}^T = \mathbf{Q} \mathbf{Y} \mathbf{Q}^T$, it is important to note that the metrics mentioned before can

easily be computed on $\mathbf{H} = \log(\mathbf{C})$. One has

$$\vartheta_G(\mathbf{C}_1, \mathbf{C}_2) = \|\log(\exp(-(1/2)\mathbf{Y}_1)\mathbf{Q}_1^T\mathbf{Q}_2\exp(\mathbf{Y}_2)\mathbf{Q}_2^T\mathbf{Q}_1\exp(-(1/2)\mathbf{Y}_1))\|_F, \quad (\text{A.2})$$

$$\vartheta_L(\mathbf{C}_1, \mathbf{C}_2) = \|\mathbf{H}_1 - \mathbf{H}_2\|_F, \quad (\text{A.3})$$

$$\vartheta_S(\mathbf{C}_1, \mathbf{C}_2) = \sqrt{\|\mathbf{Y}_1 - \mathbf{Y}_2\|_F^2 + c \|\log(\mathbf{Q}_1^T\mathbf{Q}_2)\|_F^2}. \quad (\text{A.4})$$

Appendix B. Euclidean mean in 2D

The Euclidean mean—connected to the Euclidean metric—is one of the most commonly used measures to determine the expectation of a real-valued symmetric random tensor. For instance, the arithmetic mean is suitable in determining the mean of a random diagonal matrix, $\mathbf{Y}_s(\omega_s) \in \text{Sym}(d)$ from Eq. (14)—the case of random scaling only. However, as we know that the Euclidean distance does not satisfy all the desired properties of a metric listed in Section 2, the metrics like ϑ_G and ϑ_L are hence considered to be more appropriate. We also come across the other downside of using the arithmetic mean when rotational uncertainty is incorporated into the modelling scenario, such as the random tensor $\mathbf{H}_r(\omega_r) \in \text{Sym}(d)$ in Eq. (17). That is, the Euclidean mean of $\mathbf{H}_r(\omega_r)$ does not converge to the corresponding reference tensor $\widehat{\mathbf{H}}_r$, in other words, the Euclidean mean gets distorted. Such a result is shown for the 2D case, $d = 2$.

Let us re-represent the random rotation matrix $\mathbf{R}(\omega_r) \in \text{SO}(2)$ given in Eq. (36) as

$$\mathbf{R}(\omega_r) = \begin{bmatrix} R_{11}(\omega_r) & R_{12}(\omega_r) \\ R_{21}(\omega_r) & R_{22}(\omega_r) \end{bmatrix}, \quad (\text{B.1})$$

and similarly, the reference tensor $\widehat{\mathbf{H}}_r \in \text{Sym}(2)$ in Eq. (16) as

$$\widehat{\mathbf{H}}_r = \begin{bmatrix} \widehat{H}_r^{11} & \widehat{H}_r^{12} \\ \widehat{H}_r^{21} & \widehat{H}_r^{22} \end{bmatrix}. \quad (\text{B.2})$$

Consequently, the stochastic tensor $\mathbf{H}_r(\omega_r) \in \text{Sym}(2)$ —with random orientations only—may also be rewritten in the form:

$$\mathbf{H}_r(\omega_r) = \mathbf{R}(\omega_r)\widehat{\mathbf{H}}_r\mathbf{R}(\omega_r)^T = \begin{bmatrix} H_r^{11}(\omega_r) & H_r^{12}(\omega_r) \\ H_r^{21}(\omega_r) & H_r^{22}(\omega_r) \end{bmatrix}. \quad (\text{B.3})$$

From Eq. (17), the Euclidean mean of the above random tensor takes the form:

$$\mathbb{E}[\mathbf{H}_r(\omega_r)] = \mathbb{E}[\mathbf{R}(\omega_r)\widehat{\mathbf{H}}_r\mathbf{R}(\omega_r)^T] = \begin{bmatrix} \mathbb{E}[H_r^{11}(\omega_r)] & \mathbb{E}[H_r^{12}(\omega_r)] \\ \mathbb{E}[H_r^{21}(\omega_r)] & \mathbb{E}[H_r^{22}(\omega_r)] \end{bmatrix}. \quad (\text{B.4})$$

To determine the Euclidean mean of the three upper triangular components in the above matrix, let us substitute the Eqs. (B.1) and (B.2) in Eq. (B.4). Accordingly, one can expand the element $\mathbb{E}[H_r^{11}(\omega_r)]$ as

$$\begin{aligned} \mathbb{E}[H_r^{11}(\omega_r)] &= \mathbb{E}[R_{11}(\omega_r)^2]\widehat{H}_r^{11} + \mathbb{E}[R_{11}(\omega_r)R_{12}(\omega_r)]\widehat{H}_r^{21} + \\ &\quad \mathbb{E}[R_{12}(\omega_r)R_{11}(\omega_r)]\widehat{H}_r^{12} + \mathbb{E}[R_{12}(\omega_r)^2]\widehat{H}_r^{22}, \end{aligned} \quad (\text{B.5})$$

in which

$$\mathbb{E}[R_{11}(\omega_r)^2] = \mathbb{E}[\cos^2(\phi(\omega_r))] = \mathbb{E}\left[\frac{1 + \cos 2\phi(\omega_r)}{2}\right], \quad (\text{B.6})$$

$$\mathbb{E}[R_{11}(\omega_r)R_{12}(\omega_r)] = -\mathbb{E}[\sin(\phi(\omega_r))\cos(\phi(\omega_r))] = -\mathbb{E}\left[\frac{\sin 2\phi(\omega_r)}{2}\right], \quad (\text{B.7})$$

$$\mathbb{E}[R_{12}(\omega_r)^2] = \mathbb{E}[\sin^2(\phi(\omega_r))] = \mathbb{E}\left[\frac{1 - \cos 2\phi(\omega_r)}{2}\right]. \quad (\text{B.8})$$

Given the mean direction $\bar{\phi} = 0$ of the symmetric circular variable $\phi(\omega_r)$, the properties of trigonometric moments [31, 23], such as

$$\mathbb{E}[\sin 2(\phi(\omega_r))] = 0, \quad (\text{B.9})$$

$$\mathbb{E}[\cos 2(\phi(\omega_r))] = \rho_2,$$

reduce the above equations to:

$$\mathbb{E}[R_{11}(\omega_r)^2] = \frac{1}{2} + \frac{\rho_2}{2}, \quad (\text{B.10})$$

$$\mathbb{E}[R_{11}(\omega_r)R_{12}(\omega_r)] = 0, \quad (\text{B.11})$$

$$\mathbb{E}[R_{12}(\omega_r)^2] = \frac{1}{2} - \frac{\rho_2}{2}, \quad (\text{B.12})$$

where $\rho_2 \in [0, 1]$ is the population circular variance of doubled random variable $2\phi(\omega_r)$. Therefore, by substituting Eqs. (B.10)-(B.12) into Eq. (B.5), the term $\mathbb{E}[H_r^{11}(\omega_r)]$ transforms to

$$\mathbb{E}[H_r^{11}(\omega_r)] = \frac{\widehat{H}_r^{11} + \widehat{H}_r^{22}}{2} + \frac{\rho_2}{2}(\widehat{H}_r^{11} - \widehat{H}_r^{22}). \quad (\text{B.13})$$

Similarly, the component $\mathbb{E}[H_r^{12}(\omega_r)]$ is expressed in the form:

$$\begin{aligned} \mathbb{E}[H_r^{12}(\omega_r)] &= \mathbb{E}[R_{21}(\omega_r)R_{11}(\omega_r)]\widehat{H}_r^{11} + \mathbb{E}[R_{21}(\omega_r)R_{12}(\omega_r)]\widehat{H}_r^{21} \\ &\quad + \mathbb{E}[R_{22}(\omega_r)R_{11}(\omega_r)]\widehat{H}_r^{12} + \mathbb{E}[R_{22}(\omega_r)R_{12}(\omega_r)]\widehat{H}_r^{22}. \end{aligned} \quad (\text{B.14})$$

Following the properties defined in Eq. (B.9), one may define the entities in the above equation as

$$\mathbb{E}[R_{21}(\omega_r)R_{11}(\omega_r)] = \mathbb{E}[\sin(\phi(\omega_r))\cos(\phi(\omega_r))] = 0, \quad (\text{B.15})$$

$$\mathbb{E}[R_{21}(\omega_r)R_{12}(\omega_r)] = -\mathbb{E}[\sin^2(\phi(\omega_r))] = \frac{\rho_2}{2} - \frac{1}{2}, \quad (\text{B.16})$$

$$\mathbb{E}[R_{22}(\omega_r)R_{11}(\omega_r)] = \mathbb{E}[\cos^2(\phi(\omega_r))] = \frac{1}{2} + \frac{\rho_2}{2}, \quad (\text{B.17})$$

$$\mathbb{E}[R_{22}(\omega_r)R_{12}(\omega_r)] = -\mathbb{E}[\sin(\phi(\omega_r))\cos(\phi(\omega_r))] = 0. \quad (\text{B.18})$$

Inserting the Eqs. (B.15)-(B.18) in Eq. (B.14), we thus obtain:

$$\mathbb{E}[H_r^{12}(\omega_r)] = \widehat{H}_r^{12}\rho_2. \quad (\text{B.19})$$

Furthermore, the term $\mathbb{E}[H_r^{22}(\omega_r)]$ is expanded as

$$\begin{aligned} \mathbb{E}[H_r^{22}(\omega_r)] &= \mathbb{E}[R_{21}(\omega_r)^2]\widehat{H}_r^{11} + \mathbb{E}[R_{21}(\omega_r)R_{22}(\omega_r)]\widehat{H}_r^{21} \\ &\quad + \mathbb{E}[R_{22}(\omega_r)R_{21}(\omega_r)]\widehat{H}_r^{12} + \mathbb{E}[R_{22}(\omega_r)^2]\widehat{H}_r^{22}, \end{aligned} \quad (\text{B.20})$$

whose components (in reference to Eq. (B.9)) are given by

$$\mathbb{E}[R_{21}(\omega_r)^2] = \mathbb{E}[\sin^2(\phi(\omega_r))] = \frac{1}{2} - \frac{\rho_2}{2}, \quad (\text{B.21})$$

$$\mathbb{E}[R_{21}(\omega_r)R_{22}(\omega_r)] = \mathbb{E}[\sin(\phi(\omega_r))\cos(\phi(\omega_r))] = 0, \quad (\text{B.22})$$

$$\mathbb{E}[R_{22}(\omega_r)^2] = \mathbb{E}[\cos^2(\phi(\omega_r))] = \frac{1}{2} + \frac{\rho_2}{2}. \quad (\text{B.23})$$

As a result of the substitution of Eqs. (B.21)-(B.23) in Eq. (B.20) one obtains

$$\mathbb{E}[H_r^{22}(\omega_r)] = \frac{\widehat{H}_r^{11} + \widehat{H}_r^{22}}{2} + \frac{\rho_2}{2}(\widehat{H}_r^{22} - \widehat{H}_r^{11}). \quad (\text{B.24})$$

Finally, the Eqs. (B.13), (B.19) and (B.24) when substituted into Eq. (B.4) give the Euclidean mean of the stochastic tensor $\mathbf{H}_r(\omega_r)$ in the form:

$$\mathbb{E}[\mathbf{H}_r(\omega_r)] = \begin{bmatrix} \frac{\widehat{H}_r^{11} + \widehat{H}_r^{22}}{2} + & (\widehat{H}_r^{12})\rho_2 \\ \frac{\rho_2}{2}(\widehat{H}_r^{11} - \widehat{H}_r^{22}) & \widehat{H}_r^{11} + \widehat{H}_r^{22} \\ (\widehat{H}_r^{12})\rho_2 & \frac{\rho_2}{2}(\widehat{H}_r^{22} - \widehat{H}_r^{11}) \end{bmatrix}. \quad (\text{B.25})$$

It turns out that the spectral decomposition of the above matrix can be written as

$$\mathbb{E}[\mathbf{H}_r(\omega_r)] = \widehat{\mathbf{Q}}_r \widehat{\mathbf{Y}}_r' \widehat{\mathbf{Q}}_r^T = \widehat{\mathbf{H}}_r', \quad (\text{B.26})$$

where $\widehat{\mathbf{Y}}_r' \in \mathbb{R}^{2 \times 2}$ is the deformed diagonal matrix of real-valued eigenvalues (here $\widehat{\mathbf{Y}}_r' \neq \widehat{\mathbf{Y}}_r$), and $\widehat{\mathbf{H}}_r' \in \text{Sym}(2)$ is the deformed reference tensor, such that $\widehat{\mathbf{H}}_r' \neq \widehat{\mathbf{H}}_r$. Clearly, the mean orientation $\widehat{\mathbf{Q}}_r$ of tensor $\widehat{\mathbf{H}}_r$ as defined in Eq. (16) is also preserved in the tensor $\widehat{\mathbf{H}}_r'$ as shown in Eq. (B.26).

To further elaborate the difference between tensors $\widehat{\mathbf{H}}_r$ and $\widehat{\mathbf{H}}_r'$, let us reformulate the tensor $\widehat{\mathbf{H}}_r$ in the form:

$$\widehat{\mathbf{H}}_r = \widehat{\mathbf{H}}_r^{hyd} + \widehat{\mathbf{H}}_r^{dev}. \quad (\text{B.27})$$

Here $\widehat{\mathbf{H}}_r^{hyd} := \text{tr}(\widehat{\mathbf{H}}_r)/2$ and $\widehat{\mathbf{H}}_r^{dev} := \widehat{\mathbf{H}}_r - \widehat{\mathbf{H}}_r^{hyd}$ are the hydrostatic and deviatoric components of tensor $\widehat{\mathbf{H}}_r$ respectively. Similarly, one can further rewrite tensor $\widehat{\mathbf{H}}_r'$ as

$$\widehat{\mathbf{H}}_r' = \widehat{\mathbf{H}}_r^{hyd} + \rho_2(\widehat{\mathbf{H}}_r^{dev}). \quad (\text{B.28})$$

It is clear that the shape of tensor $\widehat{\mathbf{H}}_r'$ is altered by a factor of ρ_2 when compared to the tensor $\widehat{\mathbf{H}}_r$ —seen on the deviatoric part in the above equation. Therefore, if the following condition

$$\lim_{\rho_2 \rightarrow 1} \mathbb{E}[\mathbf{H}_r(\omega_r)] = \widehat{\mathbf{H}}_r. \quad (\text{B.29})$$

is satisfied i.e. by normalizing the deviatoric part of tensor $\widehat{\mathbf{H}}_r'$ by term ρ_2 in Eq. (B.28), one may say that the scaling aspect $\widehat{\mathbf{Y}}_r$ of reference tensor $\widehat{\mathbf{H}}_r$ (from Eq. (16)) is also retained in tensor $\widehat{\mathbf{H}}_r'$.

Analogous to Eqs. (B.25) and (B.26), the Euclidean mean of stochastic tensor $\mathbf{C}_{rs}(\omega) \in \text{Sym}(2)$ —with random scaling and orientation (see Eq. (24))—may also be deduced into

$$\mathbb{E}[\mathbf{H}_{rs}(\omega)] = \widehat{\mathbf{Q}}_r \widehat{\mathbf{Y}}_s' \widehat{\mathbf{Q}}_r^T = \widehat{\mathbf{H}}_{rs}', \quad (\text{B.30})$$

in which $\widehat{\mathbf{Y}}_s' \in \mathbb{R}^{2 \times 2}$ and $\widehat{\mathbf{H}}_{rs}' \in \text{Sym}(2)$ represent the distorted versions of tensors $\widehat{\mathbf{Y}}_s$ and $\widehat{\mathbf{H}}_{rs}$ respectively. Accordingly, one may re-represent the tensor $\widehat{\mathbf{H}}_{rs}'$ as

$$\widehat{\mathbf{H}}_{rs}' = \widehat{\mathbf{H}}_{rs}^{hyd} + \rho_2(\widehat{\mathbf{H}}_{rs}^{dev}). \quad (\text{B.31})$$

Here $\widehat{\mathbf{H}}_{rs}^{hyd}$ and $\widehat{\mathbf{H}}_{rs}^{dev}$ are the hydrostatic and deviatoric elements of reference tensor $\widehat{\mathbf{H}}_{rs}$. As shown in Eq. (B.29), the change in shape of tensor $\widehat{\mathbf{H}}_{rs}'$ when compared to tensor $\widehat{\mathbf{H}}_{rs}$ is normalized by satisfying the following condition:

$$\lim_{\rho_2 \rightarrow 1} \mathbb{E}[\mathbf{H}_{rs}(\omega)] = \widehat{\mathbf{H}}_{rs}. \quad (\text{B.32})$$

Appendix B.1. Special case

A special case emerges when the random tensor $\mathbf{H}_{rs}(\omega)$ —from Eq. (24)—is modelled, such that, the reference tensor $\widehat{\mathbf{H}}_{rs}$ in Eq. (23) particularly belongs to the isotropic symmetry, for instance:

$$\widehat{\mathbf{H}}_{rs} = \begin{bmatrix} \widehat{H}_{rs}^{11} & 0 \\ 0 & \widehat{H}_{rs}^{11} \end{bmatrix}, \quad (\text{B.33})$$

and the realizations belong to a lower order of material symmetry (case of varying symmetry), along with random orientations. In such a scenario, the Euclidean mean of random tensor $\mathbf{H}_{rs}(\omega)$ naturally converges to mean $\widehat{\mathbf{H}}_{rs}$ and not to distorted mean $\widehat{\mathbf{H}}_{rs}'$ i.e.

$$\mathbb{E}[\mathbf{H}_{rs}(\omega)] = \widehat{\mathbf{Q}}_r \widehat{\mathbf{Y}}_s \widehat{\mathbf{Q}}_r^T = \widehat{\mathbf{H}}_{rs}. \quad (\text{B.34})$$

References

- [1] T. Ando, C.-K. Li, and R. Mathias. Geometric means. *Linear Algebra and Its Applications*, 385:305–334, 2004.
- [2] V. Arsigny, P. Fillard, X. Pennec, and N. Ayache. Log-euclidean metrics for fast and simple calculus on diffusion tensors. *Magn Reson Med.*, 56(2):411–421, 2006.
- [3] V. Arsigny, P. Fillard, X. Pennec, and N. Ayache. Geometric means in a novel space structure of symmetric positive definite matrices. *SIAM J. Matrix Anal. Appl.*, 29(1):328–347, 2007.
- [4] D. J. Best and N. I. Fisher. Efficient simulation of the von Mises distribution. *Applied Statistics*, 28(2):152, 1979.
- [5] A. Bóna, I. Bucataru, and M. A. Slawinski. Coordinate-free Characterization of the Symmetry Classes of Elasticity Tensors. *Journal of Elasticity*, 87(2–3):109–132, 2007.
- [6] J. R. Cardoso and F. S. Leite. Exponentials of skew-symmetric matrices and logarithms of orthogonal matrices. *Journal of Computational and Applied Mathematics*, 233(11):2867–2875, 2010.

- [7] S. C. Cowin and M. M. Mehrabadi. On the identification of material symmetry for anisotropic elastic materials. *The Quarterly Journal of Mechanics and Applied Mathematics*, 40:451–476, 1987.
- [8] J. A. Davidson, S. Gir, and J. P. Paul. Heat transfer analysis of frictional heat dissipation during articulation of femoral implants. *Journal of Biomedical Materials Research*, 22(S14):281–309, 1988.
- [9] S. R. Davidson and D. F. James. Measurement of thermal conductivity of bovine cortical bone. *Medical Engineering & Physics*, 22(10):741–747, 2000.
- [10] S. R. de Groot and P. Mazur. *Non-Equilibrium Thermodynamics*. Dover, New York, N.Y., 1984.
- [11] M. Dekking. *A modern introduction to probability and statistics: understanding why and how*. Springer texts in statistics. Springer, London, 2005.
- [12] G. Dhondt. *The Finite Element Method for Three-Dimensional Thermomechanical Applications*. Wiley, 2004.
- [13] K. Engø. On the BCH-formula in $\mathfrak{so}(3)$. *BIT*, 41(3):629–632, 2001.
- [14] G. Fishman. *Monte Carlo: Concepts, Algorithms, and Applications*. Springer Series in Operations Research and Financial Engineering. Springer-Verlag, New York, 1996.
- [15] J. I. Fujii and Y. Seo. On the Ando–Li–Mathias mean and the Karcher mean of positive definite matrices. *Linear and Multilinear Algebra*, 63(3):639–649, 2015.
- [16] D. Groisser, S. Jung, and A. Schwartzman. Geometric foundations for scaling-rotation statistics on symmetric positive definite matrices: Minimal smooth scaling-rotation curves in low dimensions. *Electronic Journal of Statistics*, 17:1092–1159, 2017.
- [17] J. Guilleminot and C. Soize. Non-Gaussian positive-definite matrix-valued random fields with constrained eigenvalues: application to random elasticity tensors with uncertain material symmetries. *Int. J. Numer. Methods Eng.*, 88(11):1128–1151, 2011.
- [18] J. Guilleminot and C. Soize. Generalized stochastic approach for constitutive equation in linear elasticity: a random matrix model. *Int. J. Numer. Methods Eng.*, 90(5):613–635, 2012.
- [19] J. Guilleminot and C. Soize. On the statistical dependence for the components of random elasticity tensors exhibiting material symmetry properties. *J. Elasticity*, 111(2):109–130, 2013.
- [20] J. Guilleminot and C. Soize. Stochastic model and generator for random fields with symmetry properties: application to the mesoscopic modeling of elastic random media. *Multiscale Model. Simul.*, 11(3):840–870, 2013.
- [21] J. Guilleminot and C. Soize. Itô SDE-based generator for a class of non-Gaussian vector-valued random fields in uncertainty quantification. *SIAM J. Sci. Comput.*, 36(6):A2763–A2786, 2014.

- [22] A. Gupta and D. Nagar. *Matrix Variate Distributions*. Monographs and Surveys in Pure and Applied Mathematics. Taylor & Francis, 1999.
- [23] S. R. Jammalamadaka and A. Sengupta. *Topics in circular statistics*. Number v. 5 in Series on multivariate analysis. World Scientific, River Edge, N.J, 2001.
- [24] S. Jung, A. Schwartzman, and D. Groisser. Scaling-rotation distance and interpolation of symmetric positive-definite matrices. *SIAM J. Matrix Anal. Appl.*, 36(3):1180–1201, 2015.
- [25] C. Malgrange, C. Ricolleau, and M. Schlenker. *Symmetry and Physical Properties of Crystals*. Springer Netherlands, Dordrecht, 2014.
- [26] A. Malyarenko and M. Ostoja-Starzewski. Statistically isotropic tensor random fields: Correlation structures. *Mathematics and Mechanics of Complex Systems*, 2(2):209–231, 2014.
- [27] A. Malyarenko and M. Ostoja-Starzewski. Spectral Expansion of Three-Dimensional Elasticity Tensor Random Fields. In *Engineering Mathematics I*, volume 178, pages 281–300. Springer, Cham, 2016.
- [28] A. Malyarenko and M. Ostoja-Starzewski. A Random Field Formulation of Hooke’s Law in All Elasticity Classes. *Journal of Elasticity*, 127(2):269–302, 2017.
- [29] A. Malyarenko and M. Ostoja-Starzewski. Tensor Random Fields in Continuum Mechanics. In *Encyclopedia of Continuum Mechanics*, pages 1–9. Springer, Berlin, Heidelberg, 2018.
- [30] A. Malyarenko and M. Ostoja-Starzewski. *Tensor-Valued Random Fields for Continuum Physics*. Cambridge University Press, 1 edition, 2019.
- [31] K. V. Mardia and P. E. Jupp. *Directional statistics*. Wiley series in probability and statistics. J. Wiley, Chichester ; New York, 2000.
- [32] N. Metropolis and S. Ulam. The Monte Carlo Method. *Journal of the American Statistical Association*, 44(247):335–341, 1949.
- [33] F. Mezzadri. How to generate matrices from the classical compact groups. *Notices of the American Mathematical Society*, 54(5):592–604, 2007.
- [34] M. Moakher. Means and averaging in the group of rotations. *SIAM J. Matrix Anal. Appl.*, 24(1):1–16, 2002.
- [35] M. Moakher. A differential geometric approach to the geometric mean of symmetric positive-definite matrices. *SIAM J. Matrix Anal. Appl.*, 26(3):735–747, 2005.
- [36] F. Nielsen and R. Bhatia, editors. *Matrix Information Geometry*, Berlin, 2013. Springer.
- [37] J. F. Nye. *Physical properties of crystals: their representation by tensors and matrices*. Clarendon Press ; Oxford University Press, 1984.
- [38] M. Ostoja-Starzewski. *Microstructural Randomness and Scaling in Mechanics of Materials*. Chapman and Hall/CRC, Aug. 2007.

- [39] A. Schwartzman. *Random ellipsoids and false discovery rates: Statistics for diffusion tensor imaging data*. PhD thesis, Stanford University, 2006.
- [40] A. Schwartzman. Lognormal Distributions and Geometric Averages of Symmetric Positive Definite Matrices: Lognormal Positive Definite Matrices. *International Statistical Review*, 84(3):456–486, 2016.
- [41] I. E. Segal and R. A. Kunze. *Integrals and Operators*. Springer, Berlin, 2nd edition, 1978.
- [42] C. Soize. A nonparametric model of random uncertainties for reduced matrix models in structural dynamics. *Probabilistic Engineering Mechanics*, 15(3):277–294, July 2000.
- [43] K. Yosida. *Functional Analysis*. Springer, 6th edition, 1980.
- [44] E. S. Zelenov. Experimental investigation of the thermophysical properties of compact bone. *Mechanics of Composite Materials*, 21(6):759–762, 1986.